IN VITRO TOXICITY OF SILVER NANOPARTICLES IN HUMAN LUNG EPITHELIAL CELLS

THESIS

Christina R. Kearns, Captain, USA

AFIT/GWM/ENP/09-M02

DEPARTMENT OF THE AIR FORCE
AIR UNIVERSITY

AIR FORCE INSTITUTE OF TECHNOLOGY

Wright-Patterson Air Force Base, Ohio

AFIT/GWM/ENP/09-M02

IN VITRO TOXICITY OF SILVER NANOPARTICLES IN HUMAN LUNG EPITHELIAL CELLS

THESIS

Presented to the Faculty

Department of Engineering Physics

Graduate School of Engineering and Management

Air Force Institute of Technology

Air University

Air Education and Training Command

In Partial Fulfillment of the Requirements for the

Degree of Master of Science in Combating Weapons of Mass Destruction

Christina R. Kearns, MS

Captain, USA

March 2009

AFIT/GWM/ENP/09-M02

IN VITRO TOXICITY OF SILVER NANOPARTICLES IN HUMAN LUNG EPITHELIAL CELLS

Christina R. Kearns

Captain, USA

Approved:

David A. Smith (Chairman)	4 Mar 2009 Date
Charles A. Bleckmann (Member)	4 Mar 09 Date
Saber Hussain (Member)	4 March 09 Date
Kyung O. Yu (Member)	5 Mar 09 Date

Abstract

Nanotechnology is quickly becoming incorporated into everyday products and uses. Silver nanoparticles, specifically, are being used in commercial products, to include aerosols. The purpose of this research was to determine whether silver nanoparticles are toxic to human lung epithelial cells. Different types (coated vs. uncoated), concentrations (10, 50, 100, and 200 μg/mL) and sizes (coated 5 and 80nm, uncoated 10 and 80nm) of silver nanoparticles were used during this study. Toxicity measurements were completed through *in vitro* techniques. Another study was also completed on toxicity mechanisms by measuring the reactive oxygen species (ROS) generated. Results showed that silver nanoparticles induce mitochondrial toxicity through a size and concentration dependent manner. Increasing the concentration yielded increased toxicity and the smaller the size induced increased toxicity to the mitochondria. Results also showed that the uncoated nanoparticles were also more toxic to the cells than the coated nanoparticles. The small nanoparticles (coated 5, uncoated 10nm) induced more formation of the ROS than the larger nanoparticles (80nm).

Acknowledgments

I would like to express my sincere appreciation to my research advisors, Drs. Kyung Yu and Saber Hussain from the Air Force Research Laboratories (RHPB) for all their advice and assistance throughout the research time that I spent in the lab. Their insight and help has been invaluable to both this thesis and for my future. I would, also, like to thank my faculty advisor, Lt. Col. David A. Smith, for his guidance and support throughout the course of this thesis effort. Finally; I thank my fiancé, who has stood beside me throughout it all.

Christina R. Kearns

CPT, USA

This Note is not to be included with the Acknowledgments – it is for information only: ***It is prohibited to include any personal information in the following categories about U.S. citizens, DOD Employees and military personnel: social security account numbers; home addresses; dates of birth; telephone numbers other than duty officers which are appropriately made available to the general public; names, locations and any other identifying information about family members of DOD employees and military personnel.***

Table of Contents

Page

List of Figures

Figure Page

List of Tables

IN VITRO TOXICITY OF SILVER NANOPARTICLES IN HUMAN LUNG EPITHELIAL CELLS

I. Introduction

1.1. Chapter Overview

Nanoparticle research is an ever increasing scientific research interest, especially over the last couple decades. Nanoparticles and nanomaterials are quickly becoming part of everyday lives. Current applications are seen in many useful products: water filters, hair appliances, socks, wound dressings, dental bonding agents, etc. (National Nanotechnology Initiative, 2008). The Department of Defense is involved in developing the nanotechnology field. For instance, the FY08 budget allocated for the national Nanotechnology Initiative was approximately $1.5 billion, with the Department of Defense (DoD) receiving almost $487 million. The projected budget for FY09 is over $1.5 billion with a projected DoD allocation of $431 million (National Nanotechnology Initiative, 2008). Applications for Department of Defense can include the use of nanoparticles in chemical and biological defense and detection, as well as personal protective equipment. Further research in this area is needed to determine the extent nanoparticles will play in biological weapons of mass destruction (WMD) defense. However, the toxicity associated with these nanoparticles has not been evaluated thoroughly. This study links the potential

bioterrorism aspects and the toxicity of nanoparticles together while looking at the effects of the nanoparticle exposure on lung cells.

Nanoparticles are materials that measure between 1 and 100 nanometers (nm) in one dimension. Nanoscience involves investigation into learning new properties of nanosize materials (National Nanotechnology Initiative, 2008). At the nanoscale, objects behave quite differently from those at larger scales. Some nanoparticles may be toxic compared the bulk parent material. For instance, gold at the bulk scale is an excellent conductor of heat and electricity, but not of light. Gold nanoparticles, on the other hand, have the ability to absorb light; therefore creating heat that can kill unneeded cells in the human body (National Nanotechnology Initiative, 2008). This is due to the decrease in size and volume resulting increased surface area to volume ratio. The increased nanoparticle surface area can more readily interact with cells, producing harmful effects.

1.2. Problem Statement

Nanoparticle research is a new area in the scientific community and is growing significantly. Toxicity levels (observed effects or lethal concentration) have not been determined for most nanoparticles. As this research field grows, the applications of nanoparticles are increasing. Nanoparticle toxicity levels must be determined to keep the population safe.

The present study is intended to determine cell viability in the presence of silver nanoparticles. The cell viability will be assessed by determining

mitochondrial function and membrane leakage in human lung cells. Furthermore, it is intended to determine the generation of reactive oxygen species (ROS) generated by the silver nanoparticles in the A549 (American Type Culture Collection, ATCC) lung epithelial cells.

1.3. Research Questions

1. Are silver nanoparticles toxic to the A549 (ATCC) lung epithelial cells?
2. Does the exterior coating of the nanoparticles affect toxicity?
3. Does the size difference of the nanoparticles affect toxicity?

1.4. Significance of Results

The use of nanoparticles for defense and detection from weapons of mass destruction is a credible and working option for the DoD. Understanding the results of this study and how silver nanoparticles can affect human lung cells at certain levels may be able to show us how to defend against or detect weapons of mass destruction, as well as how aerosols in industrial settings may affect human lungs. Depending on the toxicity levels, nanoparticles could potentially be toxic when used for chemical or biological weapons defense and detection.

1.5. Research Focus

1. To determine the toxicity of silver nanoparticles based on size and coating in lung cell models.
2. To investigate the mechanisms of toxicity.
3. Predict toxicity from *in vitro* to *in vivo* by using kinetic modeling approach.

1.6. Methodology

1.6.1. Nanoparticles

Table 1 shows the different nanoparticles used during this study. The nanoparticles were received from Clarkson University. The nanoparticles are either: coated or uncoated. The coated nanoparticles have a polysaccharide coating. The specifics of the polysaccharide coating are not known. These two categories are further broken down to small ($\leq$10 nm) and large (80 nm) nanoparticles. During this study, toxicity differences were observed based on the nanoparticle concentration, coating of the nanoparticle, and the size of the nanoparticle (small vs. large).

Table 1. Experimental Nanoparticles

Silver Nanoparticles	Small	Large
Coated (polysaccharide coating)	10 nm	80 nm
Uncoated	5 nm	80 nm

1.6.2. Methods

Several methods were employed throughout this research. First and foremost was cell harvesting. During cell harvesting, A549 (ATCC) human lung epithelial cells needed during the experimental process were cultured as described in Appendix A and in accordance with the ATCC guidelines.

After completing cell harvesting, a growth curve of the cells was determined. A549 cells were grown over seven days to determine the normal

growth rate without nanoparticle interference or interaction. Along with the growth curve, the MTT (3-(4,5-Dimethylthiazol-2-yl)-2,5 diphenyltetrazolium bromide) assay was used to determine the cell viability daily. The assay was an indicator that the cells were still alive and growing throughout the growth curve period. This is a colorimetric test measuring activity of enzymes that reduce MTT for formazan. The MTT assay indicates cell viability through a yellow to purple color change, measured by a light absorbance reading at 490 nm.

After the growth rate was determined, the cells were dosed with different nanoparticle concentrations for each different nanoparticle used. The fist assay used was the MTS (3-(4,5-dimethylthiazol-2-yl)-5-(3-carboxymethophenyl)-2-(4-sulfonyl)-2H-tetrazolium, inner salt) assay. This assay is also a colorimetric method used to identify the cytotoxic potential of the nanoparticles and determine cell viability via a light absorbance reading at 490 nm.

The next assay used was the LDH (lactate dehydrogenase) assay. This assay was used to determine the cell cytotoxicity by measuring the LDH leakage across the plasma membrane. This assay also required a light absorbance reading at 490 nm.

The last assay used was the reactive oxygen species (ROS) assay. This assay measured the formation of ROS created by silver nanoparticle exposure. This assay used a fluorescence reading at an excitation wavelength of 485 ± 20nm and an emission wavelength of 528 ± 20nm.

Transmission Electron Microscopy (TEM) was completed on the different nanoparticles to obtain the mean sizes (and standard deviation) and morphology of each different type.

Dynamic Light Scattering (DLS) was used for characterization of the nanoparticle sizes and agglomeration of nanoparticles in solution.

CytoViva™ was completed to observe the nanoparticle interaction with the cell line after 24 hours of exposure.

1.7. Assumptions

1. There is a uniform distribution of silver nanoparticles dosing of the lung epithelial cells, allowing for equal exposure of the cells to the nanoparticles.
2. Cells dosed at the same concentration of silver nanoparticles each receive the same level of exposure throughout each assay.
3. *In vitro* studies can give insight to *in vivo* studies, not give an exact determination of toxicity.

The nanoparticles solutions were sonicated prior to making the dosing solutions for approximately 10-12 seconds. Also, prior to dosing the cell plates, all solutions are stirred by a vortex stirrer to ensure even distribution in the solution.

In vitro studies can only show correlation with *in vivo* studies, but cannot replace an experimental study that is done using *in vivo* techniques. They can show some correlation to each other. Both types of studies are compared during in the literature review (Chapter 2).

1.8. Implications

This study provides toxic or biological properties of silver nanoparticles based on their physicochemical properties. The results will give insight to the material scientists to synthesize biocompatible and safe nanomaterials by modifying surface properties.

1.9. Document Overview

This paper studies the toxicity of silver nanoparticles in human lung epithelial cells. It includes the use of several different assays to determine the toxicological effects on the cell line: mitochondrial activity assay, membrane leakage assay, and reactive oxygen species assay. Each type of assay was completed at least three times for statistical significance. The assays are described in Chapter 3. The results of the assays and characterizations are found in Chapter 4. Conclusions drawn from this study are found in Chapter 5.

II. Literature Review

2.1. Background

This chapter addresses the relevance of nanoparticles to bioterrorism detection and defense, to include historical bioterrorism. The chapter also discusses nanoparticle characteristics and toxicity, followed with more specifics on silver nanoparticles used in this research. It also addresses several applications that may be associated with nanoparticles, to include possible use as aerosols. Each assay used during this experiment is also discussed.

2.1.1 Bioterrorism

Biological weapons are easier to develop, more lethal, inexpensive to produce, easier to deliver and the risk of detection is low as compared to chemical and nuclear weapons (Radosavljevic V. B., 2007). These properties create the appeal of bioweapons to terrorists. There are already many historical instances of the use of biological weapons, to include: 1) 14th Century Tartar besiegers were said to have catapulted plague infected corpses into the city of Kaffa, 2) smallpox contaminated blankets were given to Pro-French Indians by Lord Jeffery Amhurst, 3) *Salmonella typhimurium* poisoning of salad bars by the Rajneeshe Cult in Oregon in 1984, 4) Texan laboratory technician poisoned 12 of her fellow worker by inoculating *Shigella dysenteriae* into muffins and doughnuts in the staff room (Spencer, 2007).

In 1972, the Biological and Toxin Weapons Commission (BTWC) placed restrictions on the use of biological materials or chemicals that can be linked to bioweapons or chemical weapons (Lee, Hadjipnanaysis, & Parker, 2005). The

BTWC restricted the research of biological weapons to defensive research only; no offensive research was to be done thereafter.

Although, the BTWC restricted offensive research of bioweapons, there is belief that there are countries developing these types of weapons. In fact in 1998, the US Commission on National Security in the 21st Century determined that biological agents were the most likely choice of weapons for rogue states (Radosavljevic & Jakovljevic, 2007). Sadly, the U.S. has seen that this prediction was accurate during the anthrax attacks of 2001. During the aftermath of the anthrax attacks there has been a focus on weapons of mass destruction, especially the biological and chemical weapons realms. The anthrax attacks brought forth an old concern of weapons that have not been used in current times, at least not in the United States.

It can be difficult to talk about a bioweapon without defining the term. A bioweapon has been defined as the use of micro-organisms or the products of living organisms (toxins) cause damage on a population (Spencer, 2007). The population affected can include people, animals and crops. The use of these same micro-organisms as weapons can result in a major negative impact on a nation's physical, psychological or economic well-being (Spencer, 2007). This was seen throughout the timeframe of the anthrax attacks. Nanoparticles could fall within this bioweapon category. Although they are not living organisms, as discussed later, they can be products of many natural processes.

2.1.2. Nanoparticles and Bioterrorism Defense

While the discussion of bioterrorism continues, nanoparticles will have their place in the development of combating future weapons. Nanoparticles are abundant in nature. They are produced in many natural methods, to include: photochemical reactions, volcanic eruptions, forest fires, and simple erosion, plants, and animals (Buzea & Blandino, 2007). In future research the manipulation of these very small particles to defend against chemical or biological weapons will be a focus. Can they be effectively used to defend against all routes of exposure (inhalation, ingestion or dermally absorbed)? Or even used to predict exposure in the field?

The DoD has begun research to start answering these questions and has a nanotechnology defense program. The long term objective for DoD in the nanotechnology defense programs is: 'to discover and exploit unique phenomena at these dimensions to enable novel applications enhancing war fighter and battle systems capabilities' (Department of Defense, 2007). In 2002 the U.S. Army Research Office contracted with the Massachusetts Institute of Technology (MIT) to found the Institute for Soldier Nanotechnologies (ISN) (Massachusetts Institiute of Technology, 2008). This partnership was originally contracted for five years, but has been extended for another five years. The mission of the ISN is 'to create better survivability materials to protect today's Soldiers', specifically using nanomaterials (Massachusetts Institiute of Technology, 2008). The ISN addresses the questions from the previous paragraph and has been working on the development of better chemical and

biological weapons defense equipment. ISN has a Strategic Research Area (SRA) dedicated to the Chemical/Biological Materials Science with a focus in Detection and Protection (Massachusetts Instituite of Technology, 2008). This shows that research in this field has already expanded to the DoD, making further research in nanoparticles possible and important to the warfighter.

2.2. Nanoparticles

2.2.1. Overview

Nanoparticles, as defined earlier, are particles with at least one dimension less than 100 nm. Nanoparticles have a large surface area that can interact with the environment. For instance, a size reduction from 10 microns to 10 nanometers will increase the contact surface area by 10^9 (Pal, Tak, & Song, 2007). This increases the contact surface area with which the particle can interact with other matter: tissues, organs, and cells, for instance. In Figure 1, the photo shows how a nanoparticle size compares to other objects. According to Figure 1, a strand of hair is 100,000 times the width of a nanometer, knowing this can put nanoparticle experiments into a relative perspective.

Figure 1. Scale of Nanoparticles Compared to Other Objects (from http://www.nano.gov/html/facts/nanoscale.html)

As the industrial use of nanoparticles increases, so do the opportunities for biological interaction of the nanoparticles to human cells. This interaction may be dermal, through ingestion, or through inhalation. This study looks mainly at the inhalation concern, but also considers the other two areas and they will be discussed later in this chapter through the examples of previous studies. Knowing the effects through these routes may give some insight into predicting the effects on human lung cells. Most studies of silver nanoparticle toxicity are *in vitro* studies as opposed to *in vivo* studies. Although this is the case, an *in vivo* study will also be discussed later in the chapter.

2.2.2. Silver Nanoparticles

Silver has been used extensively for its antimicrobial properties in wound dressings in order to fight infection as it is a safe, inorganic antibacterial agent. Silver (including its ions and compounds) has been researched thoroughly for toxicity, which in extremely small concentrations is nontoxic to human cells (Pal, Tak, & Song, 2007). Silver (and its ions and compounds) is capable of killing about 650 types of disease-causing microorganisms (Raffi, Hussain, Bhatti, Akhter, Hameed, & Hasan, 2008). Although nano-silver is highly toxic to microorganisms, it shows a low toxicity toward mammalian cells. Raffi, et al. (2008) calls nano-silver 'oligodynamic' due to its ability to exert a bactericidal effect at minute concentrations.

A study by Raffi, et al. (2008) conducted tests on the antibacterial properties of nanosilver. They observed the growth of *Escherichia coli (E. coli)* under differing concentrations of silver nanoparticles. Silver nanoparticles in

concentrations greater than 60 μg/mL were found to be effective bactericides (Raffi, et al., 2008). Essentially, no growth of the *E. coli* was observed in trials with a concentration greater than this. The number of remaining colony forming units (CFUs) was inversely related to the concentration of silver nanoparticles.

In another study, scientists conducted an *in vivo* toxicology study of silver nanoparticle effects on zebrafish embryos. According to Berger (2008), the researchers determined that silver nanoparticles have a high probability to induce health and ecotoxicity issues in a concentration dependent mode. They found that in concentrations greater that 50 μg/mL nanosilver treated embryos showed visible signs of defects and altered physiological functions (slower heart rate, axial curvatures and body part function loss) (Berger, 2008) (Asharani, Wu, Gong, & Valiyaveettil, 2008). It was not established, though, that silver nanoparticles crossed the blood-brain barrier of the embryos.

In both studies, the *E. coli* and zebrafish embryo studies, the findings showed similar silver nanoparticle concentrations that exhibited toxic effects. These toxic level concentrations (60 μg/mL and 50 μg/mL, respectively) are within a close proximity. The greater concentration was found in the *in vitro* study and the lower in the *in vivo* study, showing some correlation with the *in vitro* and *in vivo* toxicity studies.

In other studies, silver nanoparticle interactions with mitochondria have been observed. Silver nanoparticles have been shown to be linked to decreasing mitochondrial activity in cells (Chen & Schluesener, 2008). This is important since mitochondria are often referred to as the powerhouse of the cell. They

produce the energy required for the cell to function. The cristae (inner mitochondrial folds) and the matrix are involved in, and have different responsibilities, during the energy producing functions of the mitochondria. Figure 2 shows a picture of a mitochondrion and its parts. The cristae (the inner folds of the mitochondria) and the inner membrane contain the molecules that serve as the electron-transport chain during aerobic respiration (Fox, 2006). This chain donates the electrons to the oxygen in the final oxidation-reduction reaction in the electron-transport chain. The mitochondria are also involved in the formation of the reactive oxygen species in cells. Reactive oxygen species will be discussed in depth in section 2.6.4.

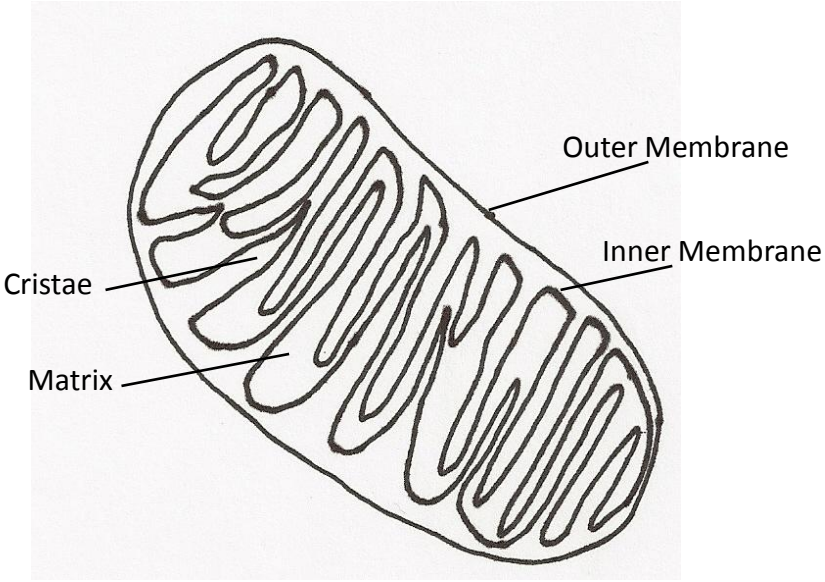

Figure 2. Cell Mitochondria

Silver nanoparticles are considered cytotoxic and cell exposure is considered to be an early step in apoptosis. The mechanism(s) linked to silver nanoparticle cytotoxicity is not completely understood. Raffi et al. (2008) suggest that, in the study of *E. coli*, bacteria change membrane morphology producing a significant increase in permeability affecting proper transport through the plasma membrane. They observed that the silver nanoparticles penetrated into the bacteria causing damage by interacting with phosphorus and sulfur containing compounds, like DNA, and resulting in cell death (Raffi, Hussain, Bhatti, Akhter, Hameed, & Hasan, 2008).

Chen and Schluesener (2008) agreed that silver nanoparticle interaction with the thiol groups of the mitochondrial inner membrane occurs. They indicated that this leads to the depletion of the antioxidant defense mechanism which, in turn, led to the formation of ROS. The ROS accumulation leads to an inflammatory response. The cells' inflammatory response initiated the destruction of mitochondria, which provoked the release of apoptogenic factors that induce cell death (Chen & Schluesener, 2008).

Supporting these studies is a study by Hussain et al. (2005) who looked at toxic response of silver nanoparticles (15 and 100 nm) in BRL 3A rat liver cells. They found that silver nanoparticles induce a toxic response in this cell type. Also, they determined that mitochondrial function diminished considerably in cells exposed to silver nanoparticles at 5-50 µg/mL (Hussain, Hess, Gearhart, Geiss, & Schlager, 2005). It was also determined that there was significant LDH leakage across the membrane in cells exposed to silver nanoparticles from 10-50

μg/mL (Hussain, et al., 2005). It was observed that along with the reduced mitochondrial membrane potential, there was an increase in ROS levels suggesting that the cytotoxicity of nanosilver was probably mediated through oxidative stress (Hussain, et al., 2005). Also, the team observed that there was an increase in ROS generation with an increase in nanoparticle concentration. The study showed that after an exposure of 24 hours, the cells showed a concentration dependent LDH leakage with significant cytotoxicity at 10-50 μg/mL (Hussain, et al., 2005). This team not only studied silver nanoparticles, but also other nanomaterials (MoO_3, Al, Fe_3O_4, and TiO_2). They determined through the use of MTT and LDH assays that the silver nanoparticles were more toxic than the other nanomaterials noted above.

2.3. Health and Safety

Silver has a high degree of use in the medical field. Severe side effects are a rare occurrence from silver poisoning, which is one reason for its common medical usage. When silver poisoning does occur, it only occurs in chronic history of silver exposure (Chen & Schluesener, 2008). As its use as nanoparticles increases, the study of the silver nanoparticle interaction in the human body becomes of greater importance as well as the different routes of exposure. Also, as the use of nanoparticles in the medical field increases, so does the probability of the silver nanoparticles interacting with human organs, tissues, and cells (Chen & Schluesener, 2008). There are few studies of how

silver nanoparticles interact with the different biological entities (organs, tissues and cells) of the human body.

A case in point is the use of silver salt. Silver salt commonly has been used in bone cement. In a 2004 study, the scientists looked at how silver salt fought infections as opposed to how silver nanoparticles fought bacteria (Alt, et al., 2004). Silver salts in polymethylmethacrylate (PMMA) bone cement were found to be highly cytotoxic to osteoblasts (bone cells), but could still fight off infections. After using the silver nanoparticles, many of the infections were reduced along with the reduction of the cytotoxic effects to osteoblasts. Figure 3 shows the differences in the cytotoxicity and antibacterial effects of the different types of silver. As can be observed, the silver salts have both high antibacterial properties and high cytotoxic effects: whereas, the silver nanoparticles have high antibacterial effects and low cytotoxicity. According to this study, the silver nanoparticles are the better material to use since they show the lowest cytotoxicity to osteoblasts.

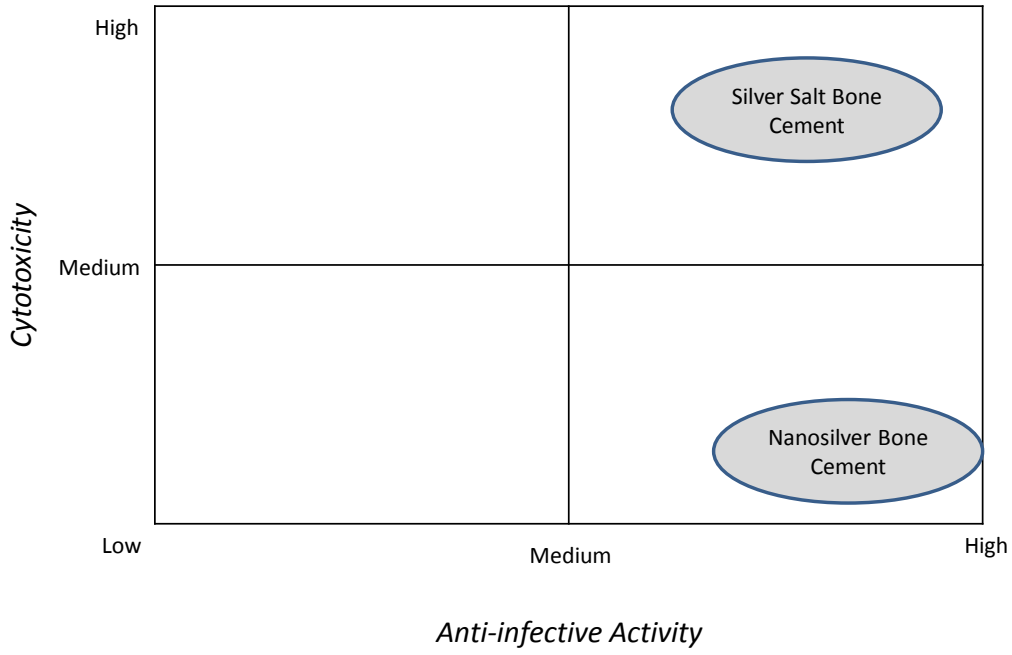

Figure 3. Overview of Cytotoxicity and Antibacterial Properties of Silver Salts versus Nanosilver Use in Bone Cement (modified from Alt, et al., 2004)

Silver nanoparticles can also be ingested into the body. Ingestion is a common route of intake. Silver nanoparticles are found in 'health maintainers' or 'immuno-boosters', water disinfection products and food stabilization products (Chen & Schluesener, 2008). These uses have increased the amount of silver nanoparticles available to be ingested by the population. Increased ingestion increases the availability of distribution of the nanoparticles to the cells. This may also lead to a greater formation of ROS in cells, which, as stated earlier, can lead to cell death. Without knowing the effects of the nanoparticles extensively, the lethal limit cannot be known. Ingesting chronic doses of silver can lead to

argyria whose most striking symptom is a bluish-grey skin color (Goyer & Clarkson, 2001).

The concern for this study is the inhalation exposure effects. With the increase in the industrial production, the general population involved may be exposed to nanoparticles in the air. Knowing how this affects the lung cells will be helpful in determining protective gear as well as the limits of exposure to humans.

2.4. Surface Characteristics

The most important characteristic of a nanoparticle is its small size. This small size allows for the increased surface area (to volume ratio) that is readily available for reactions (Chen & Schluesener, 2008). It also allows for greater particle mobility in the environment and the body. The small size gives way for different entry points into the body: ingestion, inhalation, and/or dermal absorption. With respect to inhalation, the small size allows for the particulates to make it through the nasal-pharyngeal region to the alveolar region of the respiratory system. Particles smaller than 2.5 microns, generally, are able to traverse into this region. Nanosilver may be able traverse through the nasal pharyngeal region into the alveolar region. Once in this region, nanoparticles can be distributed throughout the body (via the circulatory system, for example) where they can initiate different types of tissue responses, such as: cell defense activation, ROS generation, inflammation, and possibly cell death (Chen & Schluesener, 2008). Chen also states that several studies have shown that the

after inhalation of minute silver nanoparticle concentrations, the concentration in the lungs diminishes quickly. Silver nanoparticles were consequently detected in the blood and other organs (heart, liver, kidney, and brain) (2008). This is an indicator of how quickly nanosilver can be distributed through the body from the respiratory system to the circulatory system after inhalation.

The nanoparticles used during this research are either 'coated' or 'uncoated'. According to Dr. Kyung Yu (2008) it is expected that the 'uncoated' nanoparticles are more toxic to cell mitochondrial activity than the respective 'coated' nanoparticles. The previous research on other nanoparticles has shown that this is the case with the different nanoparticles that they have tested (Yu, 2008). The 'coated' nanoparticles have a protective coat surrounding each nanoparticle. In this study, the 'coated' nanoparticles are coated with polysaccharides.

2.5. Nanotoxicity and Bioterrorism

Nanoparticles can be inhaled, like aerosols. Aerosols can move through the nasal-pharyngeal region, bronchial region, into the alveolar region, depending on size. After inhalation, nanoparticles can deposit throughout the entire respiratory tract, starting in the nose and the pharynx, down to the lungs (Buzea & Blandino, 2007). Larger particles will naturally deposit in the nose and pharynx, or at the branch points in the respiratory system. The smaller particles, less than 2.5 microns, may make it through the lungs and alveolar region. With nanoparticles, as small as they are, they can easily move into the alveolar region.

The alveolar region has a very large surface area for nanoparticles to interact upon. If these small nanoparticles move to the alveolar region, they can be circulated throughout the body. They can then be found distributed through to the heart, blood and other organs. Nanoparticles also can be found inside cells after entering a biological entity (like organs). Once inside the cells, they can enter the cytoplasm, mitochondria, lipid vesicles, the nucleus and other organelles. Cellular uptake and capability to form oxidative products depend on the particular nanoparticle chemistry, size and shape (Buzea & Blandino, 2007). They can cause cell damage or even cell death. In Figure 4, the different pathways that nanoparticles may follow once inside the cells can be observed.

Nanoparticles not only can be inhaled, but also can penetrate through dermal barriers or be ingested to enter the circulatory systems. Dermal exposure can come through wound dressings. In a wound dressing, there is direct access into the body through the wound. Once foreign entities enter into the circulatory system, they can affect any part of the body, including the heart and the brain. One concern for the ingestion of nanoparticles is through water contamination. Animal ingestion of such contaminated products that have used these contaminated systems can pose a threat potential to the population.

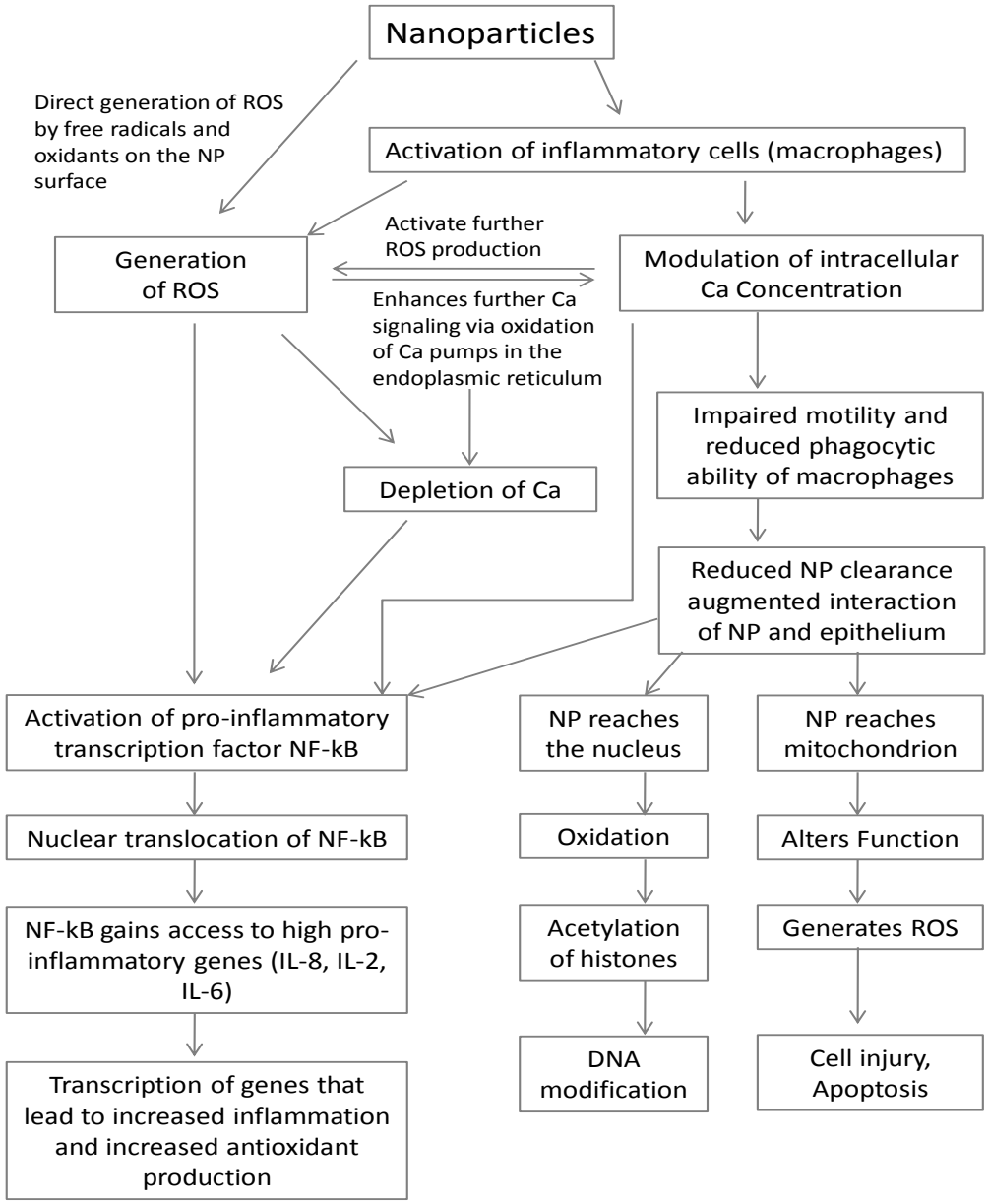

Figure 4. Schematics of the molecular events by which nanoparticles (NP) exert their toxic effects at the cellular level (modified from Buzea & Blandino, 2007)

2.6. Cellular Assays

2.6.1. MTT Assay

The MTT (yellow MTT – (3-(4,5-Dimethylthiazol-2-yl)-2,5 diphenyltetrazolium bromide)) assay measures the formation of formazan by cells. This assay is a colorimetric test measuring the activity of enzymes that reduce MTT to formazan which indicates cell viability at an absorbance reading at 490nm. MTT also measures the cell mitochondrial activity where the reduction to formazan takes place. This conversion to formazan is often used as a measure of viable (living) cells.

2.6.2. MTS Assay

The MTS (3-(4,5-dimethylthiazol-2-yl)-5-(3-carboxymethophenyl)-2-(4-sulfonyl)-2H-tetrazolium, inner salt) assay is a colorimetric method to identify the cytotoxic potential of the nanoparticles and determine cell viability by reading the absorbance at 490nm. MTS is chemically reduced by cells to formazan which is soluble in tissue culture medium. The assay measures dehydrogenase enzyme activity found in metabolically active cells (Promega). In this chemical process, reducing compounds (NADH or NADPH) pass electrons to an intermediate electron transfer reagent that can reduce the tetrazolium product, MTS, into an aqueous, soluble formazan product. Cells rapidly cannot reduce tetrazolium products after death (Promega, 2006). The production of formazan is proportional to the number of living cells; the intensity of the produced color is a good indication of the viability of the cells (Promega). The initial color of the MTS

solution is yellow. After incubation, the purple color produced is the formazan, the indication of cell viability.

The MTS assay is being used more than MTT due to time of exposure and amount of resources required. The use of DMSO for solublization of the MTT is another reason that MTS is favored. The MTS assay requires a 96-well plate which can be used to test more concentrations at once with only 200 μL of solution needed per well. The MTT assay requires the use of either 6-well or 24-well plates to accommodate the 0.5 mL of solution needed for each well. In this study, the 6-well plates were used during the growth curve determination.

2.6.3. LDH Assay

The LDH assay is used to determine cell cytotoxicity by measuring the lactose dehydrogenase (LDH) leakage across the plasma membrane. LDH is a cytoplasmic enzyme that is released into the cytoplasm upon cell lysis (Nanotechnology Characterization Laboratory, 2006). It is considered to be a measure of membrane integrity. Cells that lose membrane integrity release lactate dehydrogenase. According to the Nanotechnology Characterization Laboratory the basis of LDH assay is that:

1) LDH oxidizes lactate to pyruvate,

2) Pyruvate reacts with the tetrazolium salt INT to form formazan, and

3) The water-soluble formazan dye is detected spectrophotometrically (2006).

The increase in the amount of formazan correlates directly to the increase in the number of lysed cells (Biovision, 2008).

2.6.4. Reactive Oxygen Species (ROS) Assay

Many studies, both *in vivo* and *in vitro*, have shown that nanoparticle toxicity can induce the formation of reactive oxygen species. Reactive oxygen species have been shown to damage cells by peroxidizing lipids, altering proteins, disrupting DNA, interfering with signaling functions and modulating gene transcription (Buzea & Blandino, 2007). Oxidative stress can be a response to cell injury. Generally, small amounts of ROS are made in the cell through physiological processes, one of which is the electron transport chain within the mitochondria. During this process, molecular oxygen is reduced one electron at a time (Boelsterli, 2007). Figure 5 shows the stepwise reduction of oxygen in cell mitochondria. Partially reduced oxygen species may break away from the usual electron transfer process within the mitochondria (Boelsterli, 2007). This creates a steady small amount of ROS inside the cell. ROS are generated within the cell to a degree through the reduction-oxidation cycling of outside entities, xenobiotics (silver nanoparticles in this study). This occurs through the separation of monooxygenases or by rerouting the electrons from the electron transport chain (Boelsterli, 2007).

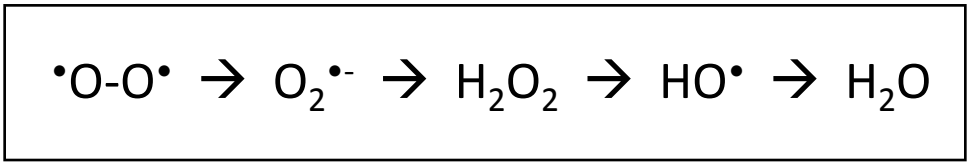

Figure 5. Stepwise reduction of oxygen (modified from Boelsterli, 2007)

Xenobiotics have been shown to increase the ROS production. They do this through penetration into the mitochondria and interfering with the electron transport chain, thus blocking normal electron flow (Boelsterli, 2007). The xenobiotics can also induce oxidative stress thereby causing the oxidation of the nucleic acids within the cell. Figure 6 shows an overview of what happens within the cell after the ROS have been formed. The ROS induce the antioxidant response of the cell, causing damage to DNA. The damaged DNA either repair themselves or cause further damage to the cells.

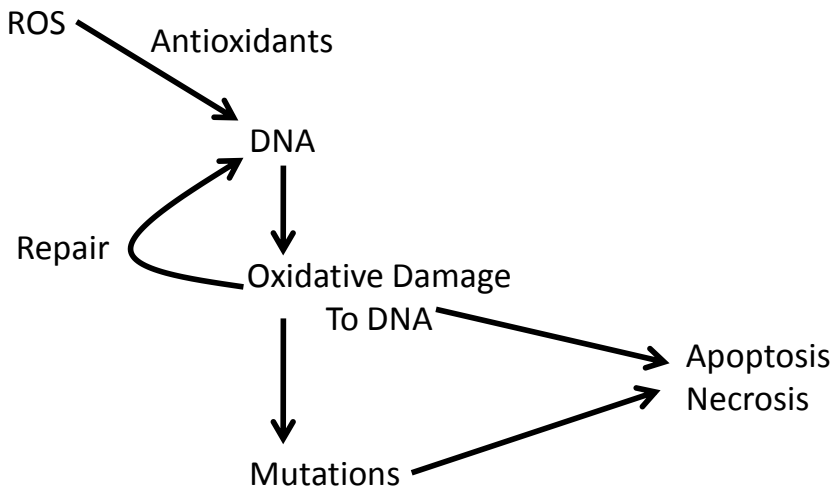

Figure 6. Oxidative DNA Damage Can Lead to Apoptosis
(Modified from Boelsterli, 2007)

Because of the mitochondria naturally generates ROS, the mitochondrial DNA is more prone to have an oxidative event that may cause permanent damage. The mitochondria also have ineffective repair mechanisms for ROS

damage. As a result of this inefficiency, the mitochondrial DNA amass more oxidatively damaged bases (Boelsterli, 2007). But there are numerous copies of mitochondrial DNA and numerous mitochondria in the cell; this far outweighs the general oxidative event that may occur to the mitochondria. When adding the additional creation of ROS through a xenobiotic it can be expected that the mitochondria will not be able to survive the mass amount of ROS production.

2.7. Current Research and Applications

Research in nanoparticles has increased dramatically over the last couple decades. While all the applications of nanoparticles will not be mentioned, the following applications show the wide array of products that nanoparticles are being used in currently.

Products using nanoscale materials now available include: anti-bacterial wound dressings (use nanoscale silver), water filtration, catalysis, dental bonding agent, step assists on vans, bumpers and catalytic converters on cars, sunscreens and cosmetics, and dry powder that can neutralize gas and liquid toxins in chemical spills and elsewhere (National Nanotechnology Initiative, 2008). Research in nanomedicine, for instance, is focused on finding new ways for diagnosing and treating disease (National Nanotechnology Initiative, 2008). Inorganic nanoparticles generally possess versatile properties suitable for cellular delivery, including a wide availability, rich functionality, good biocompatibility, potential capability of targeted delivery, and controlled release of carried drugs (Xu, Zeng, Lu, & Yu, 2006). Other uses are in carbon nanotubes (CNTs) and

nanofilms (eyeglasses, computer displays, and cameras to protect or treat the surfaces) (National Nanotechnology Initiative, 2008). Also, there is research that incorporated the use of silver nanoparticles in fighting HIV. The researchers found that silver nanoparticles undergo a size dependent interaction with human immunodeficiency virus type 1 (Pal, Tak, & Song, 2007). As seen with this example and the bone cement study, medical research is an important sector of the nanotechnology development.

There are few studies look at the interaction of silver nanoparticles and their biodistribution and organ accumulation, as well as the tissue interaction and toxicological implications (Chen & Schluesener, 2008), but the field is growing. Studies still need to be completed on the transdermal considerations of nanosilver toxicity especially since they have use in the clothing industry (socks) and the medical field (wound dressings).

Lastly, the DoD, in conjunction with the ISN, is looking at improving Soldier survivability in the field/wartime environments. The development of a suit that is self contained and can detect and protect from chemical or biological weapons of mass destruction is on their developmental horizon (PennWell Corporation, 2003).

2.8. Summary

Silver nanoparticles are beginning to, and have begun to be used in many products. Not only are these nanoparticles being used by civilians, but also, the Department of Defense has begun researching its own applications for silver and

other nanoparticles. With so few studies showing how these nanoparticles interact biologically in humans, it cannot be understood what the potential risks may be. Research of this nature can assist in the building blocks of learning how these nanoparticles may interact biologically in humans. This study begins to look at how silver nanoparticles interact with human lung cells.

III. Methodology

3.1. Introduction

The goal of this research was to determine if silver nanoparticles are toxic to human lung epithelial cells. This was carried out through *in vitro* methods that initially used MTS assays to determine mitochondrial activity and cell viability. LDH assays were used to determine the membrane leakage of the cells. ROS assays were conducted to determine the presence or evolution of reactive oxygen species in the cell line. Each assay required cell culturing and splitting prior to starting. Therefore, the assays were started on a day which cell splitting was completed.

Each assay used a positive control solution that either was another nanoparticle solution (MTS and LDH) or hydrogen peroxide solution (ROS). The positive control was used to monitor the assays for proper readings, as well as to ensure that they were working in the method that was expected. By comparing the results of the positive control to the nanoparticle readings, it could be determined if the assay was working properly for each trial.

Each assay was completed in triplicate to conduct statistical analysis. The steps for cell culturing, growth curve determination and each separate assay are listed in detail in Appendices A-F.

Along with the assays previously listed, Dynamic Light Scattering (DLS), Transmission Electron Microscopy (TEM), and CytoViva™ characterization analyses were performed on the cells and/or the different silver nanoparticles. These results are also shown in this chapter.

3.2. Assumptions

There are several key assumptions that were made prior to the experimental process.

1. An equal distribution of silver nanoparticles occurs after cell dosing, giving equal exposure to each nanoparticle to epithelial cells.
2. Cells dosed at the same concentration of silver nanoparticles each receive the same level of exposure throughout each assay.
3. *In vitro* studies can give insight to *in vivo* studies.

3.3. Cell Lines

The cells used during this experiment were from the American Type Culture Collection (ATCC) (Manassas, VA), Number CCL-185, Designation A549. The A549 cell line is from human lung epithelial (carcinoma) cells, with an initial isolation date in 1972. These cells were chosen to look at possible inhalation exposure toxic effects upon the lungs.

3.4. Cell Culture and Splitting

A549 (ATCC) lung epithelial cells were cultured in accordance with the ATCC Protocol found in Appendix A (ATCC, 2008). One change to the ATCC protocol was to use a 5 mL rinse with Phosphate Buffer Solution (PBS) after the initial aspiration. Cell splitting was conducted every three to four days at confluence. Cell confluence was determined by observation through a light microscope.

3.4.1. Growth Curve

A549 cells were grown over a specified length of time to determine the normal growth rate of the cells without nanoparticle interference. This experiment started with a solution of 100,000 cells/mL in growth media. The cell growth was monitored over seven days. Each day the cells were counted to determine growth change from day to day using a standard hemocytometer and light microscope. Along with the cell counting, a cell viability assay was conducted. The MTT assay was used to determine the viability of the cells each day using an absorbance reading at 490 nm. The blank measurement used for this assay was acidified-isopropyl alcohol (IPA). A growth curve was determined using the data from the daily cell counts. A full outline of the procedure is found in Appendix B.

3.5. Absorbance and Fluorescence Readings

The absorbance of the materials was read on a Biotek® Synergy HT plate reader. The readings were taken at 490 nm for MTT, MTS, and LDH Assays. The ROS fluorescence was read at an excitation wavelength of 485 ± 20 nm and an emission wavelength of 528 ± 20 nm from the bottom of the plate. The results were exported into a Microsoft® Excel spreadsheet for calculations.

3.6. Nanoparticles

The nanoparticles were received from Clarkson University. The coating on the ‘coated’ nanoparticles is a polysaccharide coating. Table 2 shows the different types and concentrations of silver nanoparticles used throughout this

experiment. The nanoparticle solutions were made in exposure media. The exposure media for the MTS and LDH assays were the same. The exposure media used during the ROS assay was a colorless version of exposure media (discussed in Section 4.2.5.). These concentrations indicated in Table 2 were used during the MTS, LDH and ROS assays.

Table 2 Expe.rimental Nanoparticle Sizes and Concentrations

Nanoparticles	**Control**	**Dosing Concentrations (μg of nanoparticle per mL of solution)**			
Coated (5 nm & 80 nm)	0 μg/mL	10 μg/mL	50 μg/mL	100 μg/mL	200 μg/mL
Uncoated (10 nm & 80 nm)	0 μg/mL	10 μg/mL	50 μg/mL	100 μg/mL	200 μg/mL

In Figure 7, the nanoparticle solutions have been made for dosing 96-well plates for an assay. From left to right are: uncoated 5 nm, uncoated 80 nm, coated 10 nm, and coated 80 nm in the dilutions given above in Table 2. From closest to furthest in columns are dilutions of 10 μg/mL, 50 μg/mL, 100 μg/mL, and 200 μg/mL.

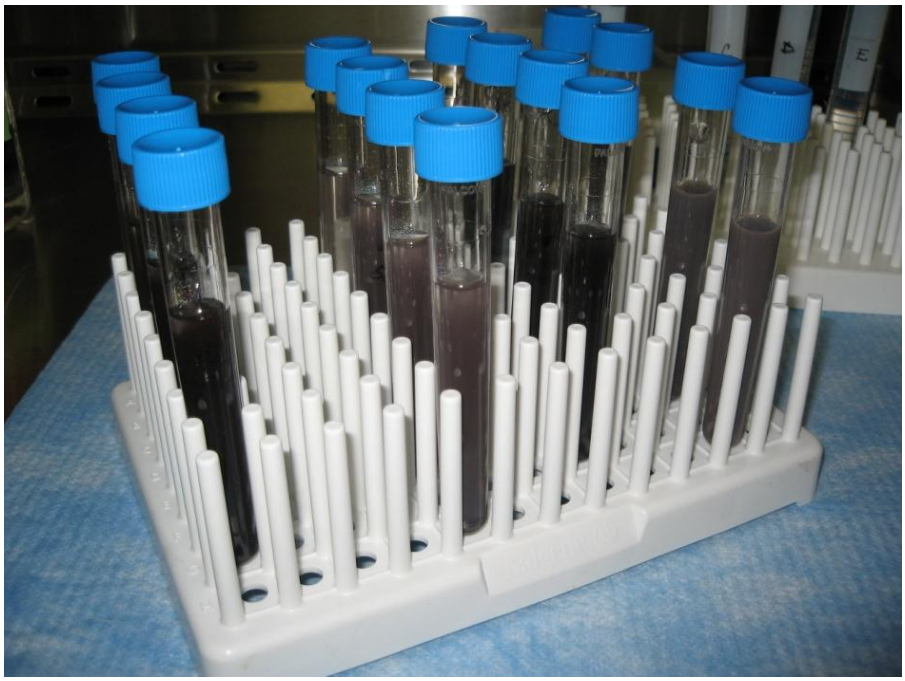

Figure 7. Nanoparticle Solutions Prepared for Dosing Plates

3.7. MTT Assay

The MTT (3-(4,5-Dimethylthiazol-2-yl)-2,5 diphenyltetrazolium bromide) assay was used to determine the viability of the cells by reading the absorbance reading at 490 nm. The control was acidified-isopropyl alcohol (IPA). It is a colorimetric test used to measure activity of enzymes that reduce MTT for formazan (yields a purple color). The initial color of the MTT solution is yellow. After incubation the reaction yields a purple color of the solution. The intensity of the color indicates the amount of viable cells. This assay was completed in accordance with Appendix C. The absorbance was read on a Biotek® Synergy HT Plate reader. The results were exported to and graphed on Microsoft® Excel software.

This assay was used during the growth curve determination. It was used to determine the viability of the cells during the growth curve only. The MTS assay was used for all calculations and determinations of cell viability during the rest of the study.

MTT solutions were kept in light protected vials in a refrigerator at 4°C. The MTT solution was made by dissolving 10 mg of MTT powder into 20 mL of PBS.

3.8. MTS Assay

The MTS (3-(4,5-dimethylthiazol-2-yl)-5-(3-carboxymethophenyl)-2-(4-sulfonyl)-2H-tetrazolium, inner salt) (Promega, 2006) assay is a colorimetric method to identify the cytotoxic potential of the nanoparticles and determine cell viability using an absorbance reading at 490 nm. The MTS solution (Promega, CellTiter 96® AQ_{ueous} One Solution Reagent) starts as a yellow solution. After incubation, dependent on the amount of viable cells, the solution changes to a purple color. The intensity indicates viability. This procedure was done in accordance with Appendix D and completed in triplicate. The control medium used was exposure media. The positive control used was a Cadmium Dioxide nanoparticle solution. The absorbance was read on a Biotek® Synergy HT Plate reader at 490 nm. The results were exported to and graphed using Microsoft® Excel software.

MTS solutions were kept in light protected vials in a refrigerator at 4°C.

3.9. LDH Assay

The LDH assay was used to determine cell cytotoxcity through measuring the lactose dehydrogenase leakage across the plasma membrane. This procedure was completed in accordance with Appendix E and the Promega® protocol. The control used was exposure media. The positive control used was a Cadmium Dioxide solution in exposure media. The absorbance was read at 490 nm on a Biotek® Synergy HT Plate reader. The results were exported to and graphed on Microsoft® Excel software.

3.10. Reactive Oxygen Species (ROS) Assay

The ROS assay measures the formation of reactive oxygen species by nanoparticle interaction in the cells. The procedure references the methods used in Wang & Joseph (1999) and can be found in detail in Appendix F. This method uses DCFH-DA (2',7'– dichlolorodihydrofluorescein diacetate). The theory behind using DCFH-DA is that the non-fluorescent fluorescin derivatives will emit fluorescence after being oxidized (Wang & Joseph, 1999). During this assay, hydrogen peroxide was used as the positive control. After being applied to intact cells, the non-ionic, nonpolar DCFH-DA crosses cell membranes and is hydrolyzed enzymatically by intracellular esterases to nonfluorescent DCFH. In the presences of reactive oxygen species, DCFH is oxidized to highly fluorescent dichlorofluorescein (DCF) (Wang & Joseph, 1999).

The fluorescence of the cells was read on a Biotek® Synergy HT plate reader. The excitation filter was set at 485 ± 20 nm and the emission filter was

set at 528 ± 20 nm and set to read the plate from the bottom. The results were exported to and graphed on Microsoft® Excel Software.

3.11. Dynamic Light Scattering and Transmission Electron Microscopy

Transmission electron microscopy (TEM) characterization was performed to obtain nanoparticle size and morphology on a Hitachi H-7600 tungsten-tip instrument at an accelerating voltage of 100 kV. Nanoparticles were examined after suspension in water (1 mg/mL) and subsequent deposition onto formvar/carbon-coated TEM grids (~10 µL). Image J was used to measure nanoparticles after TEM imaging with proper scale calibration. Information on mean size and standard deviation was calculated from measuring over 100 nanoparticles in random fields of view in addition to images that show general morphology of the nanoparticles. Mr. Craig Murdock performed all TEM measurement analysis during this research.

Dynamic light scattering (DLS) (for characterization of nanomaterial size or agglomeration of the nanoparticles in solution) was performed on a Malvern Instruments Zetasizer Nano-ZS instrument. The device uses a 4mW He-Ne 633nm laser to analyze the samples. Samples were prepared as previously described above in the TEM section and vortexed to provide a homogeneous solution, and then 1.5 mL was transferred to a square cuvette for DLS measurements. Solutions were made at a concentration of 50 µg/mL for measurement. The Malvern Zetasizer Nano-ZS uses the Dispersion Technology Software (V4.20) for data collection and analysis. The mean particle diameter is

calculated by the software from the particle distributions measured and the polydispersity index (PdI) given is a measure of the size ranges present in the solution (Malvern Instruments Ltd., 2005). The PdI scale ranges from 0 to 1, with 0 being monodisperse and 1 being polydisperse. The software calculates the PdI value from the G1 correlation function and from parameters defined in the ISO standard document 13321:1996 E. Mr. Craig Murdock performed all DLS measurement analysis during this research.

3.12. CytoViva™

After counting the cells, a solution of 150,000 cells/mL was made in growth media. One milliliter of the solution was added to each half of a two-chamber polystyrene vessel culture slide, tissue culture treated glass slides (BD Falcon). The slides were then incubated for 24 hours at 37°C.

After 24 hours of incubation, the slides were aspirated and washed with 1mL of PBS. A 10 μg/mL dosing solution was prepared for each nanoparticle type (Uncoated 5 nm and 80 nm; Coated 10 nm and 80 nm). One milliliter of each nanoparticle solution was added to the appropriate slide. The slides were then incubated for 24 hours. One milliliter of exposure media (F-12K Medium, Kaighn's Modification of Ham's F-12 with 1% Penicillin/Streptomycin) was used in the control slide. The slides were then incubated for 24 hours at 37°C.

After 24 hours of incubation, the media was aspirated from the culture slides and washed with 1 mL of 1xPBS. The PBS was aspirated from the slides. Then, the chambers were removed from the slides. Seven microliters of PBS

was added to each side of the slide and covered with a cover slip. The cells were evaluated (on glass slides with cover slips) using the 60x oil lens and were imaged with an Olympus IX71 Microscope platform coupled to the CytoViva™ 150 Ultra Resolution Imaging (URI) System, as described in a study by Skebo et al. (Skebo, Grabinski, Schrand, Schlager, & Hussain, 2007). The QImaging Retiga 4000R and QCapture Pro Imaging Software 6.0 were used to capture and store images. Mr. Craig Murdock performed the CytoViva™ analysis.

3.13. Statistical Analysis

After reading either the absorbance or fluorescence, the data was downloaded to Microsoft Excel for statistical analysis. Each assay was completed in triplicate. The data was transferred to SYS-STAT (statistical software) to determine statistical changes for all data compiled for the MTS and LDH assays. Results for the ROS assay were analyzed using a one-way analysis of variance with Bonferroni multiple comparisons using SYS-9 statistical software. Statistical significance for all assays was determined using a 95% confidence interval.

IV. Data Description and Analysis

4.1. Introduction

This chapter presents the data gathered from the methodologies described in Chapter 3. The data includes: the growth curve, MTS assay (24, 48, and 72 hour trials), LDH assay (24, 48, and 72 hour trials), and ROS assay (1, 4, 6, and 24 hour trials). Also, the results from the TEM, DLS and Cyto-Viva are shown. The MTS and LDH assays show the respective combined results after 48 hours of exposure to nanoparticles. The 48 hour exposure timeframe was determined to be the most reliable time for these assays. The ROS assay data includes the time data for each nanoparticle type and the compiled time data from the three trials. The TEM, DLS, and Cyto-Viva show the nanoparticles in solution and with the A549 cell line.

After compiling the data and observing initial trends and values in Microsoft Excel, the data was entered into the SYS-STAT (MTS) or SYS-9 (ROS) program. This program performed the statistical analysis of the data sets. The *p*-value was set to $p \leq 0.05$. The SYS-STAT program was used to statistically determine significant differences between data sets. The program also identified outliers within any data sets.

4.2. Results

4.2.1. Growth Curve

The goal of the growth curve was to determine how many days it would take to grow 1,000,000 cells/mL starting with 100,000 cells/mL (in growth media).

To determine this, seven 6-well plates were seeded with 0.5 mL per well of a 100,000 cells/mL solution of A549 cells (in growth media) on day zero. There was one plate for each day for the duration of the growth curve. Each day the cells were counted and an MTT assay was performed in accordance with Appendix B. At day four, the growth media was changed in each remaining plate to ensure growth. The data for the daily cell count and log of the daily cell count is seen in Table 3. The growth curve was plotted on a logarithmic curve over seven days of growth as can be seen in Figure 8. It was determined that it would take about seven days to grow the cells by one factor of 10.

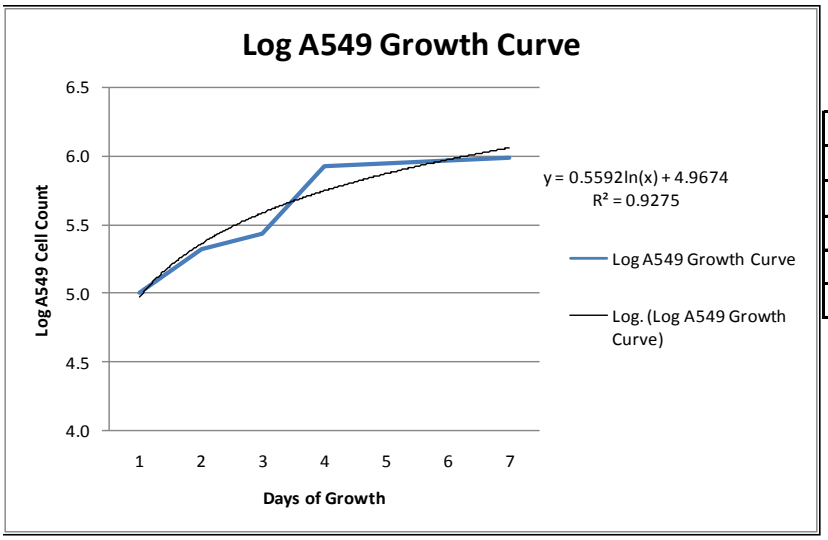

Day	Count	Log Count
1	100000	5.0000
2	205000	5.3118
3	267500	5.4273
4	830000	5.9191
7	957500	5.9811

Figure 8. Seven Day Growth Curve with Trend Line

Figure 8 shows the greatest growth rate occurred between days three and four and shows a plateau effect between days four and seven. The data for the number of cells is not known for days five and six for the number of cells, but still can be interpolated through Figure 8.

4.2.3. MTS Assay

Silver nanoparticles are known to interfere with the absorbance readings. Therefore, 80 µL of supernatant was removed from the dosed plate (from each well) and placed in new plate to read the absorbance at 490 nm without interference from nanoparticles in solution. Initially, a preliminary trial was completed at 24 hours of nanoparticle exposure, 48 hours of nanoparticle exposure, and 72 hours of nanoparticle exposure. This was done to determine the best exposure duration. It was determined from those results, that 48 hours of exposure to nanoparticles was the best fit for the amount of exposure time. Figures 9 through 11 show the data compiled from the different time trials conducted: 24, 48, and 72 hours, respectively.

The 24 hour exposure time did not show a strong response through the absorbance change from the control (% MTS reduction) during the assay. The difference from the control medium was not significant enough at this time frame at all nanoparticle solutions. Only the uncoated 5nm showed a strong change in absorbance with increasing concentration. The difference from the control was generally less than 20% reduction across the board (except with the uncoated, 5 nm – 200 µg/mL solution), as can be seen with Figure 9. This time trial also

showed variance from what was expected to occur during this assay. Instead of a steady decrease across the concentrations for each nanoparticle type, some increased with respect to percent control MTS reduction.

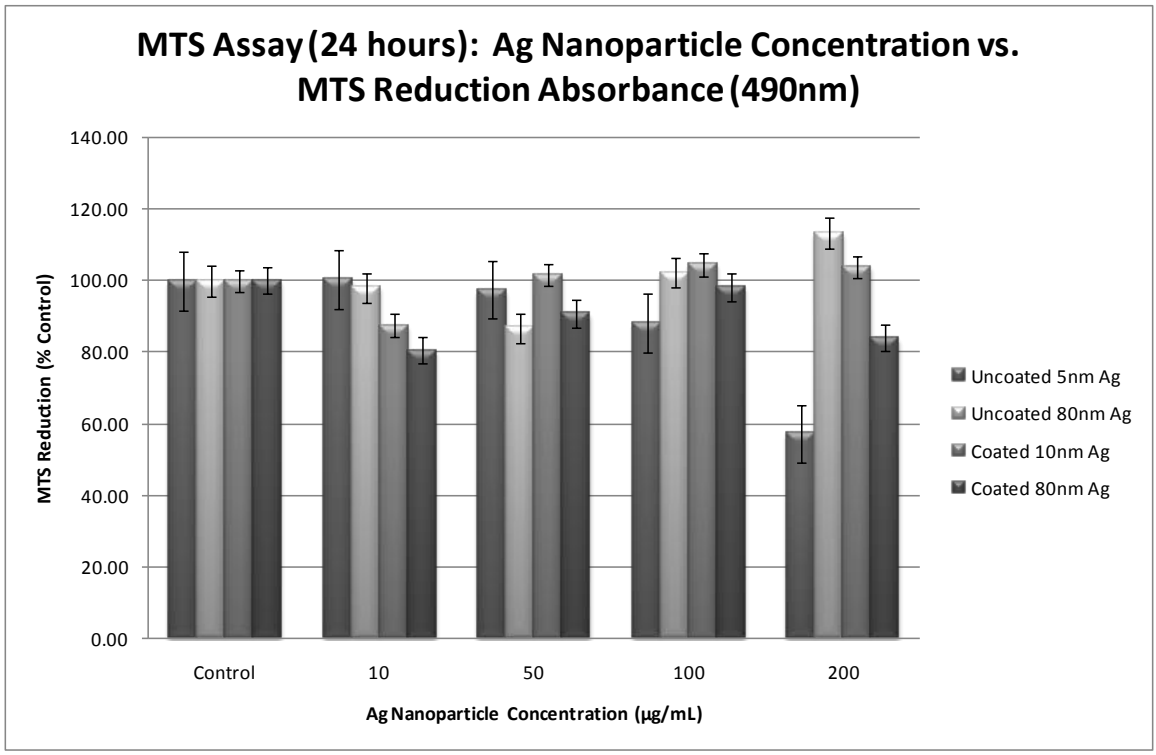

Figure 9. MTS Assay - 24 Hour Exposure

The 48 hour exposure time trial results are shown in Figure 10. The 48 hour exposure time trial showed that the lung cells were exposed to the toxic effects of the nanoparticles for the appropriate duration. There was a significant change of the toxicity over time without the cell death effect seen in the 72 hour trial. The trend showed what was expected with respect to concentration dependent toxicity; a steady decrease across increasing concentrations for each

nanoparticle. It can be observed that as the concentration of the separate nanoparticles increase, so does the toxicity to the cells. Also, in this time trial, as opposed to the 72 hour trial, there appeared to be enough viable cells remaining at all concentrations of each nanoparticle to expect that this would be the case during the further testing at this exposure duration.

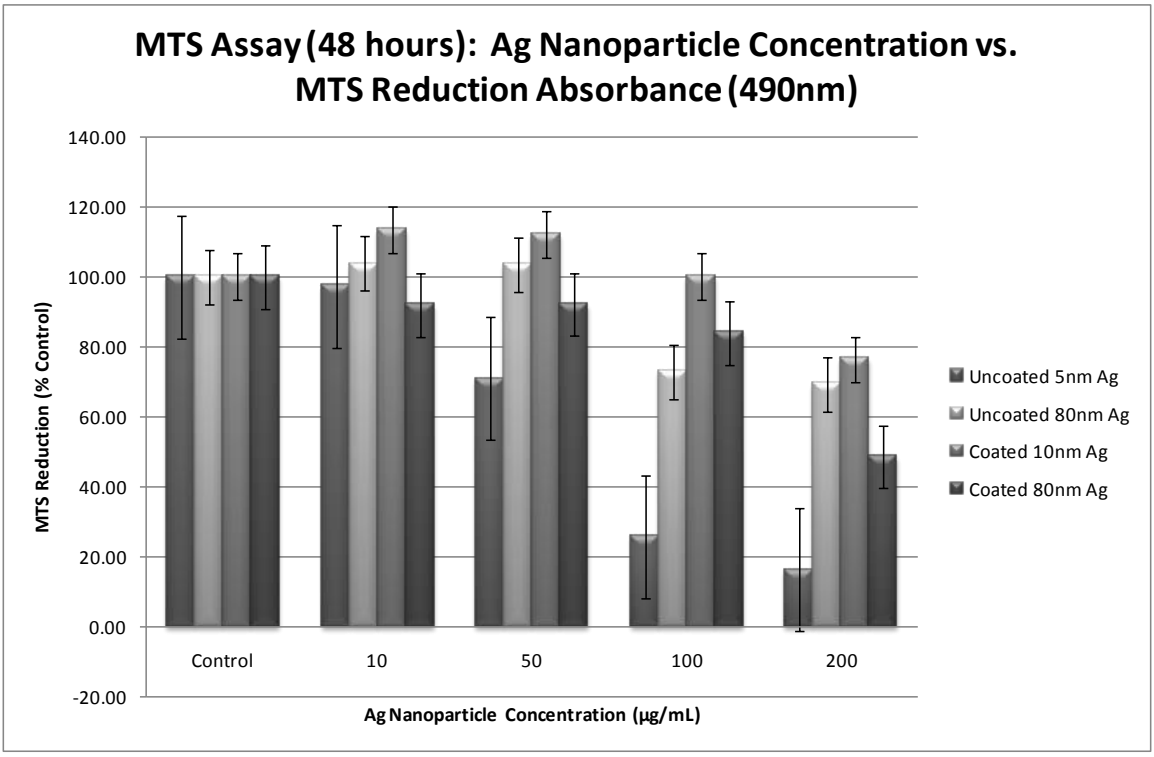

Figure 10. MTS Assay - 48 Hour Exposure

The 72 hour exposure time trial indicated that the cells received too extensive an exposure from the nanoparticles, as can be seen in Figure 11. The cells were essentially killed by the length of nanoparticle exposure at the 100 and 200 µg/mL concentrations. The 50 µg/mL concentration for both uncoated

nanoparticles sizes showed similar results, indicating cell death at this concentration. Because of this increased cell death, when compared to the other two time trials and due to exposure length, this was determined not to be the optimal duration to expose the cells to the nanoparticles.

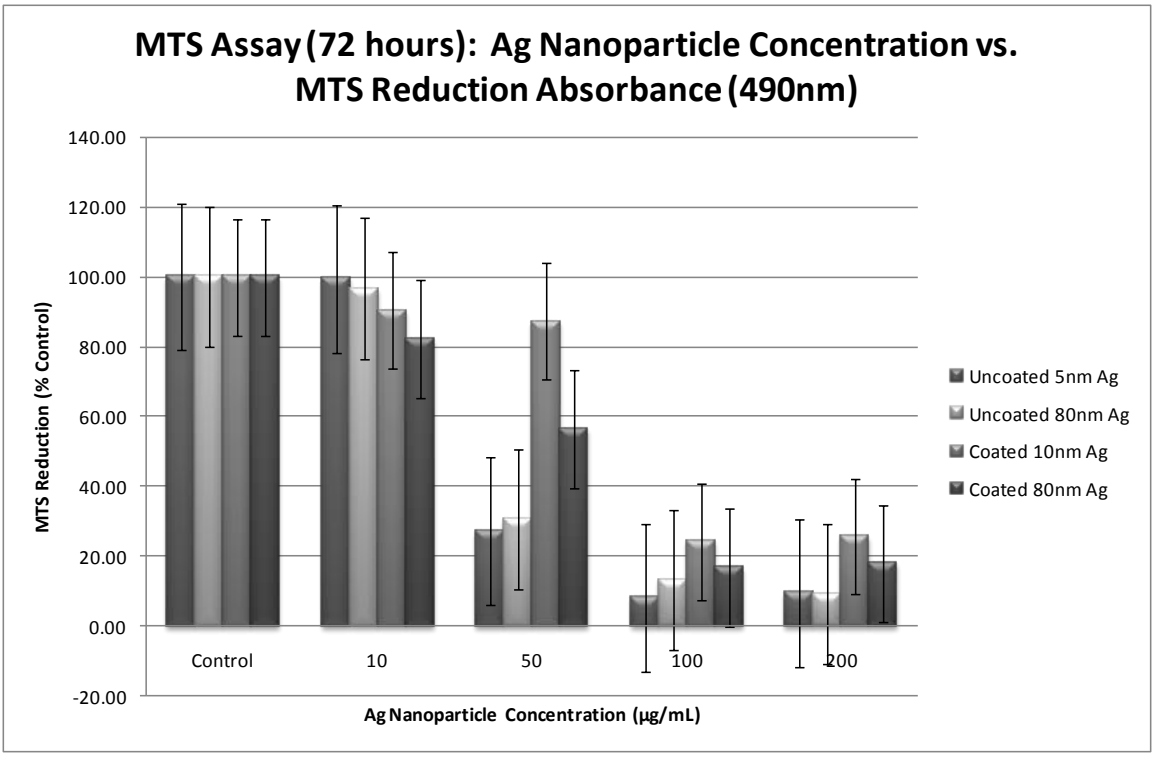

Figure 11. MTS Assay - 72 Hour Exposure

After determining that 48 hours was the best timeframe, the results were compiled from three trials at this time of nanoparticle exposure. The results from the separate trials are in Figure 12. The concentration dependence of the nanoparticle toxicity can be observed. As the concentration increases from 0 µg/mL to 200 µg/mL, the MTS reduction percentage decreases. This indicates

that the mitochondrial function of the cells decreased. This is shown through the Percent MTS Reduction of the formazan in the cells. The mitochondria were not available for the reduction, which implies that cell death had occurred.

With respect to nanoparticle size affecting toxicity, it is observed that the larger of the nanoparticles, in the coated and uncoated category, tended to be less toxic than its smaller counterpart. The uncoated 5nm silver nanoparticles showed the greatest toxicity to the human lung cells, with essentially complete cell death at 200 μg/mL concentrations. The uncoated 80nm concentrations showed less toxicity than the uncoated 5nm. The uncoated 80nm showed about 1.5 times less toxicity at the higher two concentrations than its 5nm counterpart. The coated nanoparticles, both 10nm and 80nm, showed approximately equal toxicity at the 200μg/mL concentrations. The toxicity of the coated nanoparticles remained within a range of 10% MTS reduction percentage of each other at each different concentration.

Another significant difference in the MTS reduction assay was the difference between the coated and uncoated nanoparticles. The uncoated nanoparticles clearly show more toxicity than the coated nanoparticles, as can be observed in Figure 12. With the two larger nanoparticles, 80nm, the coated remained about 15-20% greater MTS reduction than its uncoated counterpart through the differing nanoparticle concentrations. This indicated that the coated nanoparticle is less toxic to the cells than the uncoated nanoparticles.

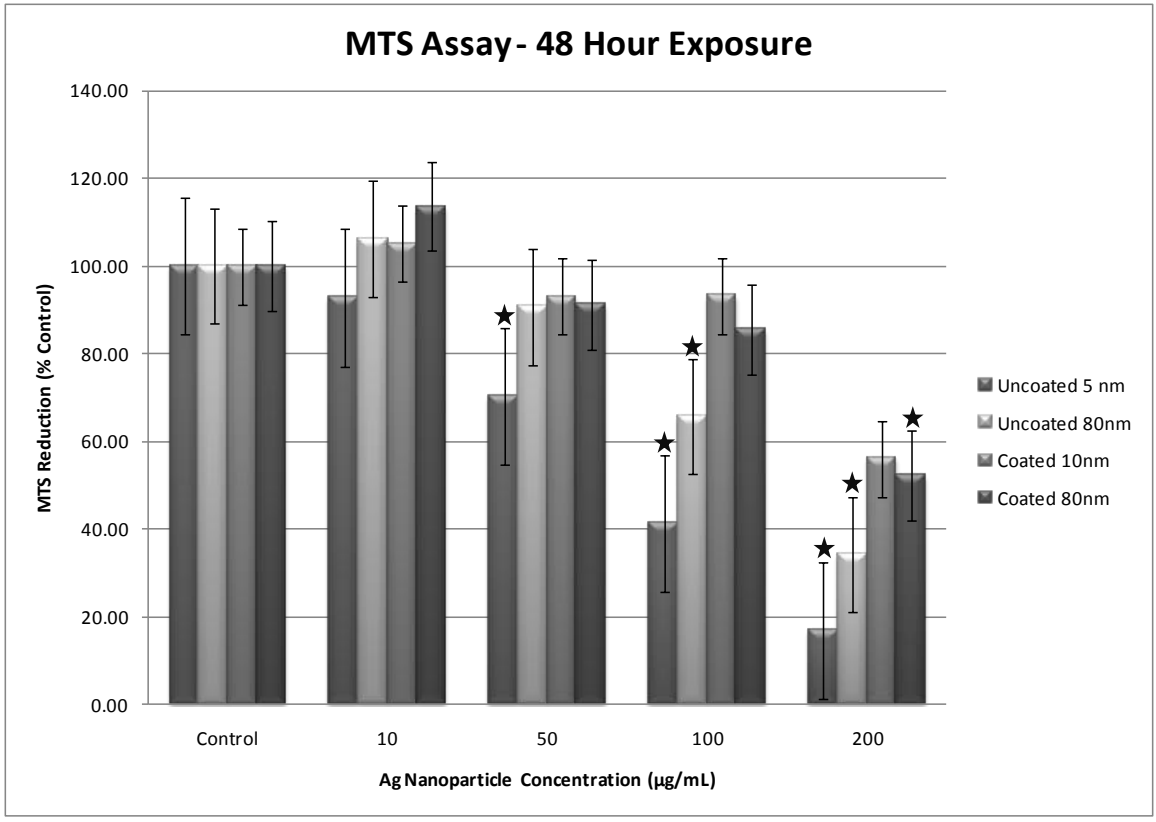

Figure 12. Combined MTS Assay Results - 48 Hour Exposure – (*) indicate statistically significant variation from the control

With the two smaller nanoparticles (5 and 10 nm), the uncoated nanoparticle (5 nm) begins with a 10% decrease difference in MTS reduction at 10 µg/mL with respect to the 10 nm coated at the same concentration. At the 50 µg/mL concentration, this difference more than doubles to almost 25% decrease difference in MTS reduction. The difference between the MTS reduction still increases at the 100 µg/mL to approximately a 40% MTS reduction decrease difference with the uncoated 5 nm showing increased toxicity with the increased concentration. The uncoated 5 nm indicated almost complete cell death by the

200 μg/mL concentration, whereas the 10nm coated indicated that about half the cells were still viable at the same concentration.

The stars indicate where there is a statistically significant difference between the results of the nanoparticle effects with respect to the control ($\rho<0.05$). The uncoated 5nm silver nanoparticles show significant toxic effects at concentrations greater than or equal to 50 μg/mL. The uncoated 80nm silver nanoparticles show significant toxicity at concentrations greater than or equal to 100 μg/mL. The coated nanoparticles, both 10nm and 80nm, require at least 200 μg/mL before significant toxicity occurs to the lung epithelial cells.

4.2.4. LDH Assay

Like the MTS assay, silver nanoparticles have shown to interfere with the absorbance readings. Therefore, 80 μL of supernatant was removed from the dosed plate (from each well) and placed in new plate to read the absorbance at 490nm without interference from nanoparticles in solution. This assay was completed in conjunction with the MTS assays. Appendix E describes the step by step instruction of this assay.

Initially, a preliminary trial was completed at 24 hours, 48 hours, and 72 hours of nanoparticle exposure. This was done to determine the best exposure duration. It was determined from those results that 48 hours of exposure to nanoparticles was to be used for the exposure duration. Figures 13 through 15 show the data compiled from the different time trials conducted: 24, 48, and 72 hours, respectively. It was expected that, if the MTS assay showed greatest toxicity at the highest concentrations (low MTS reduction); then, the LDH assay

should indicate high leakage (% LDH leakage to media) at corresponding concentrations.

The 24 hour time trial was not chosen as the optimal amount of exposure time for this assay, because the response from the absorbance was minimal. As seen in Figure 13, the leakage percentage was minimal across the nanoparticle concentrations, except for the uncoated 5 nm nanoparticles. Further exposure was needed to achieve the expected result. As the nanoparticle concentration increased, it would be expected that the LDH leakage into the media would also increase. The 24 hours of exposure time trial did not show this to be the result for all nanoparticles, as seen in Figure 13.

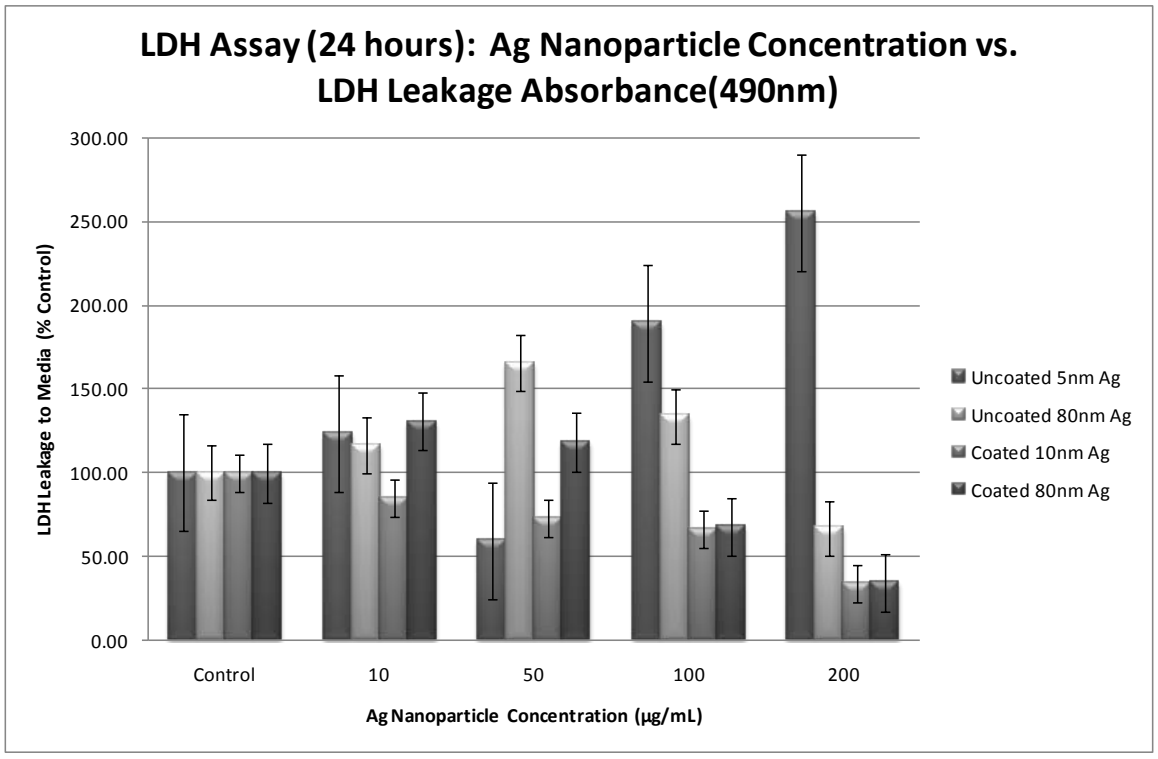

Figure 13. LDH Assay - 24 Hour Exposure

The 48 hour time trial was chosen as the amount of time to expose the lung cells. The results of this time trial are found in Figure 14. Although it still did not show the concentration dependent increase in LDH leakage, this assay was completed with the MTS assay which was completed after 48 hours of exposure. The equal time of nanoparticle exposure also was needed for an equal comparison of results between the LDH and MTS assays.

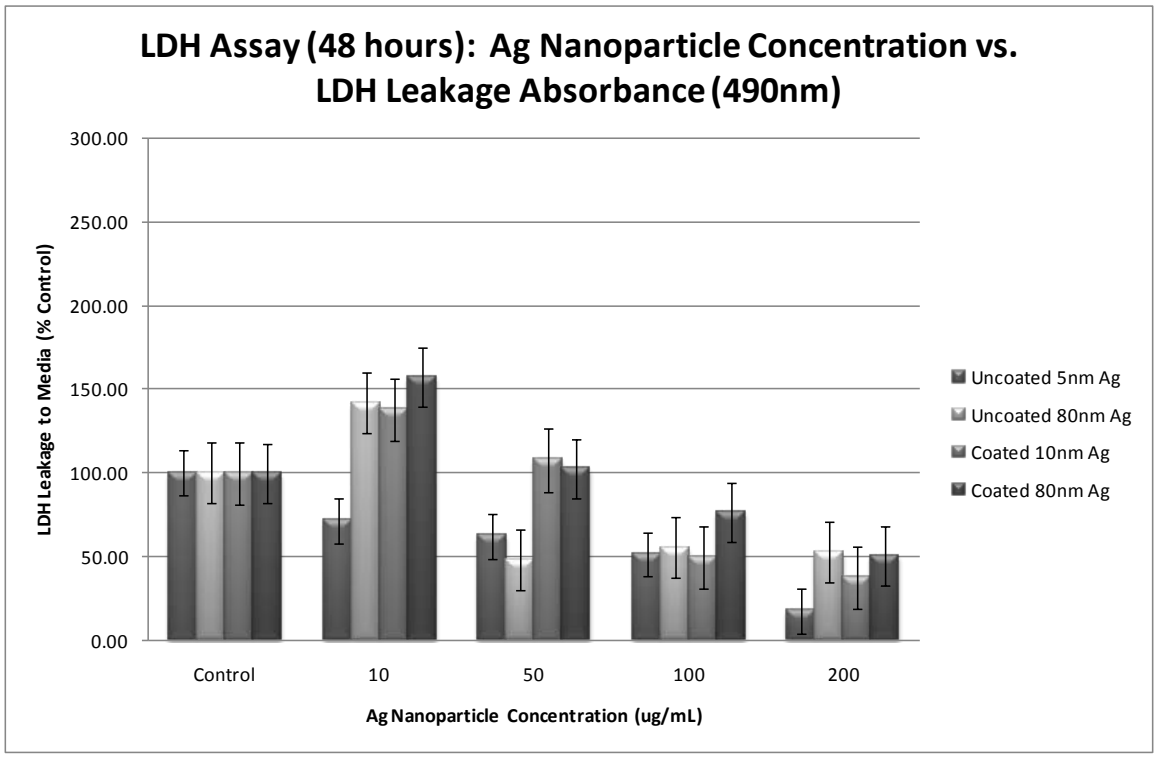

Figure 14. LDH Assay - 48 Hour Exposure

The 72 hour trial also did not show a concentration dependent increase in LDH leakage. Figure 15 shows the data from the 72 hour time trial. There was

no significant change in the absorbance at any nanoparticle concentration. This exposure time was not chosen due to this.

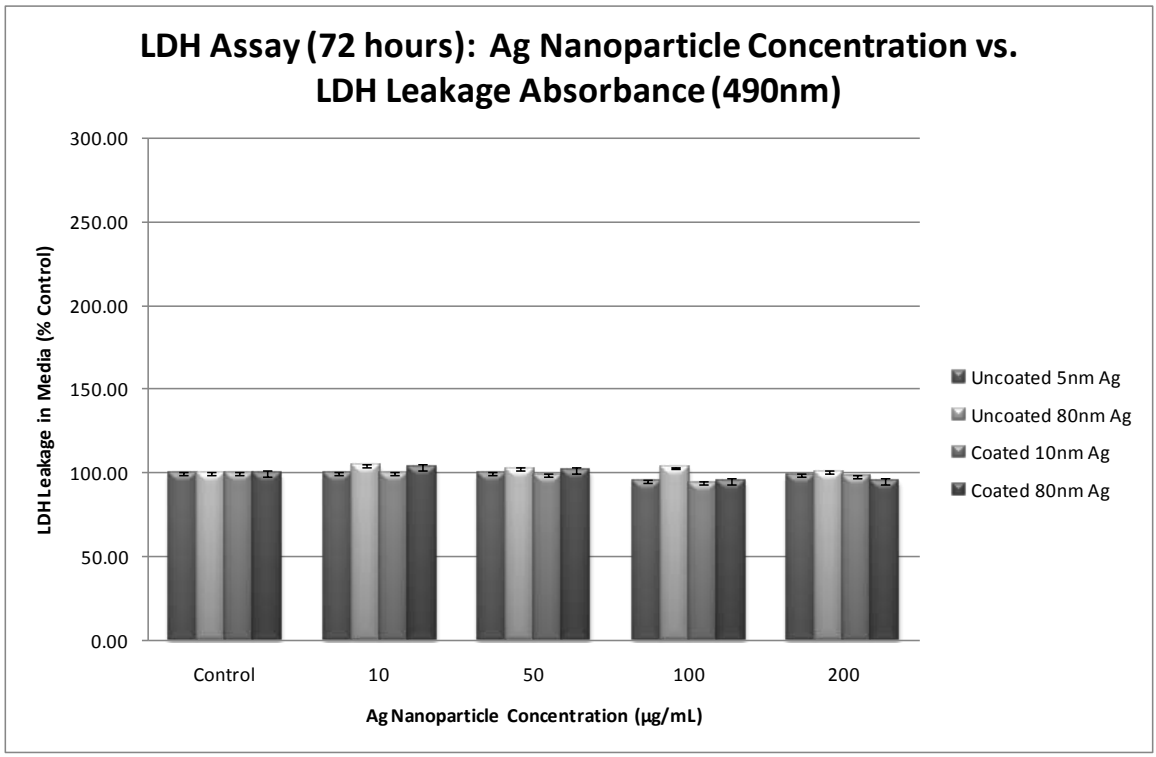

Figure 15: LDH Assay - 72 Hour Exposure

Three separate trials were completed with the 48 hour nanoparticle exposure. The 48 hour time point was chosen to have a direct comparison to the MTS assay. The results of the 48 hour exposure trials are graphed in Figure 16. Again, it was observed that the LDH leakage is decreasing across the concentrations instead of increasing. From other trials on different nanoparticles, it was expected that as the concentration of the nanoparticle solution increased, so would the percent leakage of LDH into the media. This would be an indicator of the toxicity of the nanoparticles to the cell membrane.

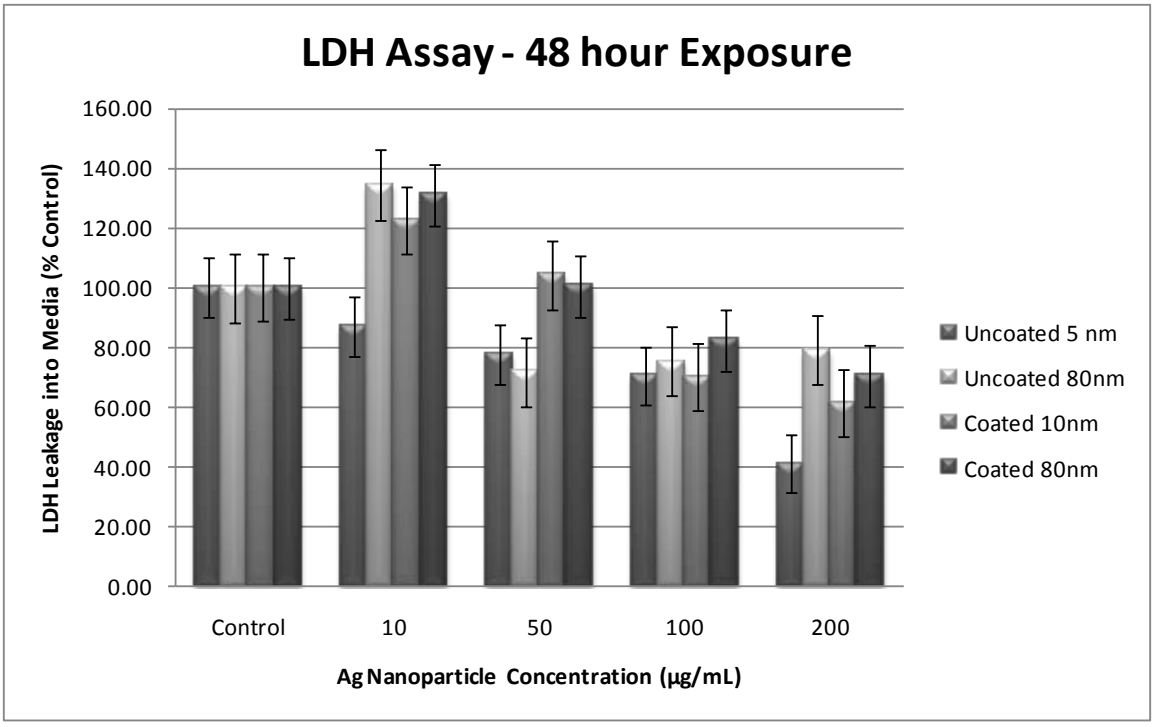

Figure 16. Combined LDH Assay Results - 48 Hour Exposure

Because the results were not what would be expected with this type of assay, it was determined that this was not a reliable assay to determine toxicity of the silver nanoparticles with this cell line. It is suspected that the nanoparticles may interfere with the LDH media or the LDH enzyme with the A549 cells. Also, it can be inferred that the silver nanoparticles are killing the lung cells; therefore there is no leakage of the LDH to the media occurring. This can be inferred while comparing the MTS results to the LDH results. It is observed through the MTS assay that there was increased cell death occurring at the higher concentrations of silver nanoparticles.

4.2.5. ROS Assay

The exposure media and growth media used for the ROS testing is different than the media used in the other assays. The media used during this testing have no phenol red coloring in them. The phenol red has been associated with interference with the fluorescence readings required for this type of testing. Therefore, in order to have a 'clean' reading, media without phenol red is needed. The details of these solution are described in Appendix F.

Trials were completed after initial dosing (0 hour), 1 hour, 4 hours, 6 hours, and 24 hours. The procedure used was adapted from in Wang & Joseph (1999) and described in Appendix F. Instead of reading the same plate for all readings as indicated in their procedure, one 96-well plate was prepared for each time point. Figure 17 shows an example of a black well plate after 1 hour of incubation.

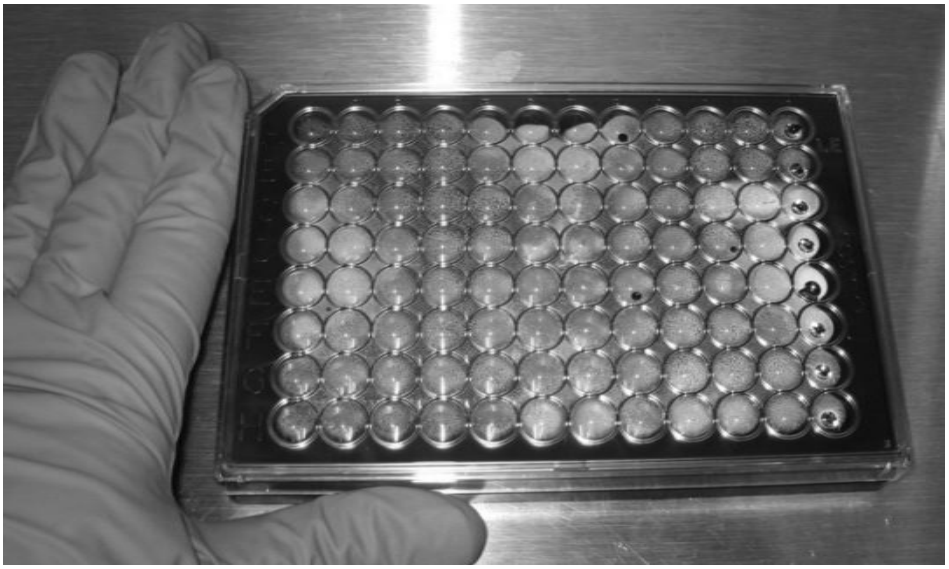

Figure 17. 96-Well Black Plate for ROS Assay after 1 Hour Incubation

After an initial fluorescence reading of each plate, 80 μL of supernatant was transferred from the original plate to a new plate to be read without the nanoparticle interference. Three trials at each time point were completed. The data was compiled by time point and each different nanoparticle type. Figures 18-21 show the compiled results of the 3 separate ROS trials by each different nanoparticle type at each time point that a reading was taken.

Figure 18 shows the results from the uncoated 5nm silver nanoparticle for the ROS assay. It shows that there is a 3-fold increase with respect to the control (fluorescence). The ROS formation peaked at this time point and steadily decreased with increase exposure time. There is also an inverse proportionality between the nanoparticle concentration and ROS formation: the lower the concentration, the higher the formation of ROS in the cell line. A higher ROS fluorescence reading is observed at the lower concentration of the uncoated 5nm than at the higher concentration. At all time points after the initial reading, fluorescence indicates that ROS have been formed at all concentrations. At 10 μg/mL, the uncoated 5nm nanoparticles show that they form ROS as quickly as one hour after dosing the cells.

After conducting statistical analysis on the data, it was determined that there were only two significant peaks; at 1 hour and with the 10 and 50 μg/mL concentrations. Other peaks did not show statistical differences. This is due to the range that the results of each (of the other) peak spanned. The standard deviation of the data and the data means did not give statistical differences with the control means.

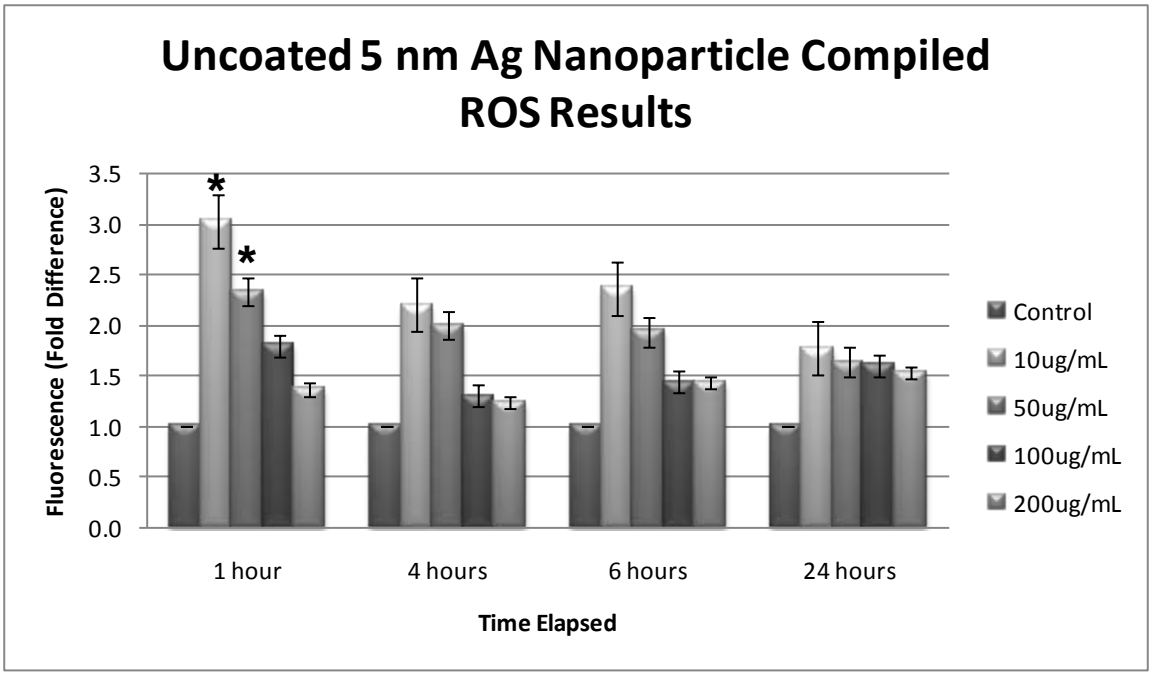

Figure 18. Reactive Oxygen Species Results for Uncoated 5 nm - (*) indicate statistically significant variation from the control

Figure 19 shows the results for the coated 10 nm silver nanoparticles. These nanoparticles do not show the same fold difference as the 5 nm silver nanoparticles; however the coated 10 nm still shows that ROS are formed after the cells are dosed with the nanoparticles. The coated 10 nm reach a peak at about 2-fold the fluorescence of the control. The coated 10 nm show its greatest fold difference with the control with the 50 μg/mL concentration at the 1 hour time points, which is the only statistically significant peak for this nanoparticle. Other peaks did not show statistical differences. This is due to the range that the results of each (of the other) peak spanned. The standard deviation of the data and the data means did not give statistical differences with the control means.

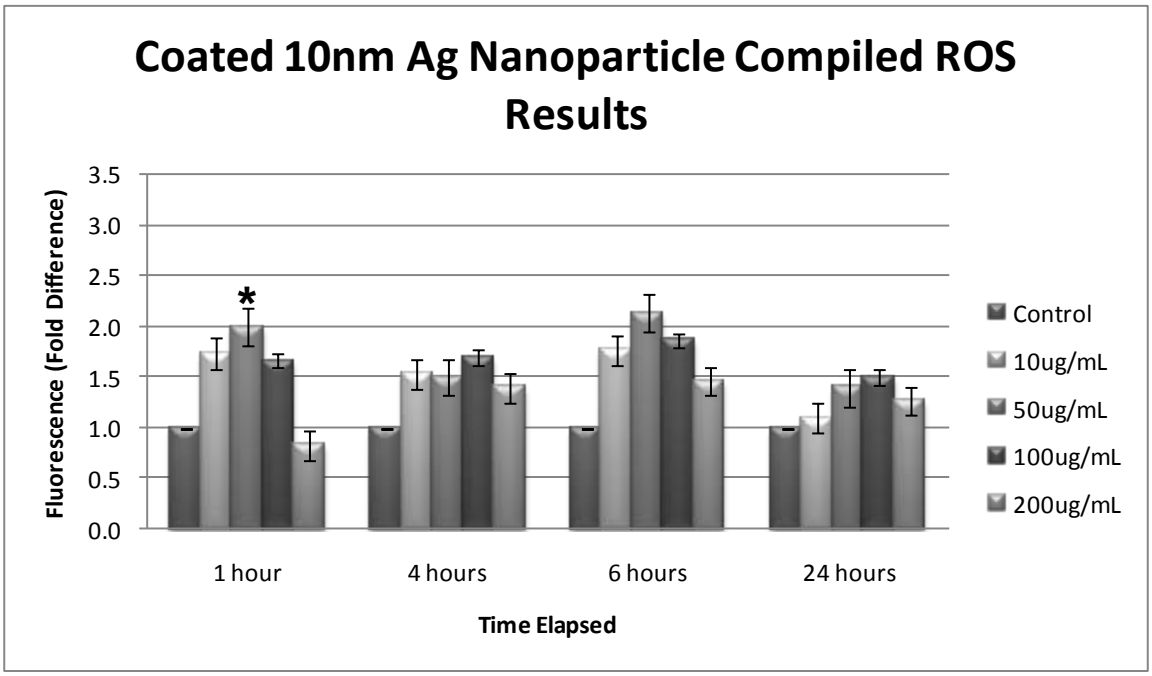

Figure 19. Reactive Oxygen Species Results for Coated 10 nm - (*) indicate statistically significant variation from the control

Figure 20 shows the results for the uncoated 80 nm silver nanoparticles. Like the uncoated 5 nm silver nanoparticles, the lowest concentration indicated that ROS formation occurred upon dosing the cells with the nanoparticle, though only slightly (about 0.2-fold difference with control). For the 10 and 50 μg/mL concentrations, the fold difference peaks out at 1.5 fold-difference (with respect to the control) at the 1 hour time point and maintain around that value for both the 4 and 6 hour time points. The higher two concentrations, 100 and 200 μg/mL, show peak fold-difference at the 24 hour time point. At the higher concentrations, it is observed that it takes longer to have significant change in ROS concentration than with the lower concentration of the same nanoparticle.

The only significant peak was at the 10 μg/mL with one hour of exposure. Other peaks did not show statistical differences. This is due to the range that the results of each (of the other) peak spanned. The standard deviation of the data and the data means did not give statistical differences with the control means.

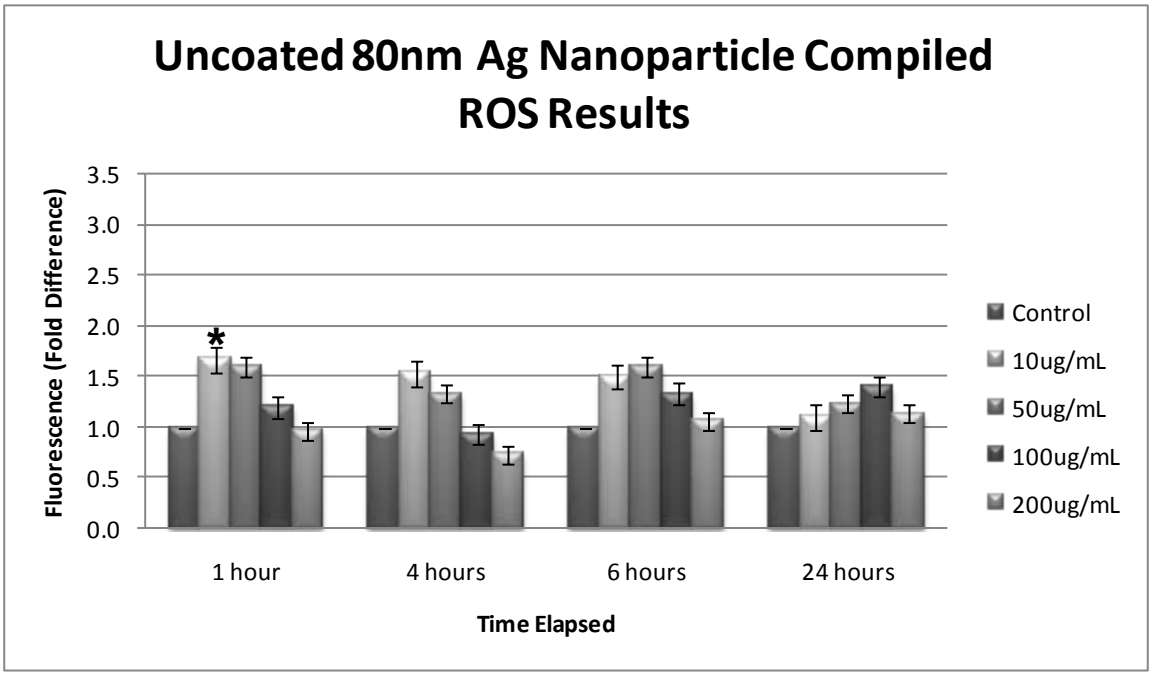

Figure 20. Reactive Oxygen Species Results Uncoated 80 nm - (*) indicate statistically significant variation from the control

Figure 21 shows the results for the coated 80 nm silver nanoparticles. The 80 nm coated nanoparticles show similar ROS formation results compared with the uncoated 80 nm silver nanoparticles. Both 80 nm silver nanoparticles show similar levels in ROS formation during the trials. They both have shown similar maximums and minimums at the different time points. The larger

nanoparticles (80 nm) show less toxicity than the smaller respective nanoparticles (5 and 10 nm).

After conducting statistical analysis on the data, it was determined that there were no significant peaks. Other peaks did not show statistical differences. This is due to the range that the results of each (of the other) peak spanned. The variation of the data means did not give statistical differences with the control means.

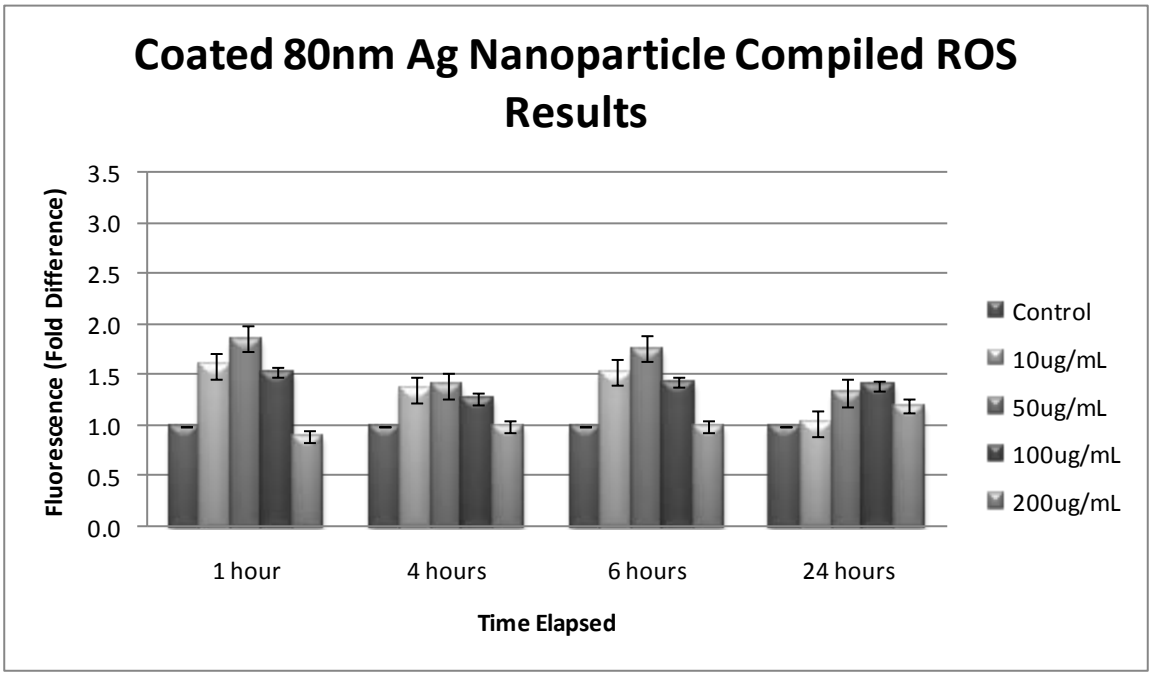

Figure 21. Reactive Oxygen Species Assay Results for Coated 80 nm

Overall, the ROS assay indicates that the formation of ROS in the A549 cell line is dependent on nanoparticle size and concentration. The uncoated 5

and coated 10 nm nanoparticles show a higher formation of ROS than either of the 80 nm nanoparticles. This is an indication that the smaller nanoparticles are more toxic than the larger respective nanoparticles. The concentration of the nanoparticles affects the ROS formation. With the 5 nm nanoparticles, the lowest concentration shows the highest ROS formation; the ROS formation (toxicity) decreases with an increasing concentration of the nanoparticle. Similarly, the coated 10 nm has the highest ROS formation at 50 μg/mL, then the levels of ROS formation decrease with increasing concentration.

After statistical analysis, no peaks for the coated 80nm silver nanoparticles were determined to be statistically significant.

The statistical analysis for the ROS assay data were analyzed using a one-way analysis of variance with Bonferroni multiple comparisons (Rosner, 1990). The statistical analysis was completed by Dr. Latha Narayanan using SYS-9 software and a confidence interval of 95% ($\rho \leq 0.05$).

4.3. Dynamic Light Scattering and Transmission Electron Microscopy

Figure 22 shows the TEM primary particles size and distribution determined from measurement of over 100 particles from random fields of view. Dynamic Light Scattering (DLS) results are shown in Table 4. DLS z-average particle diameter in solution and LDV zeta potential measurements were measured at sample concentrations of 50 μg/mL of each different nanoparticle used in this study.

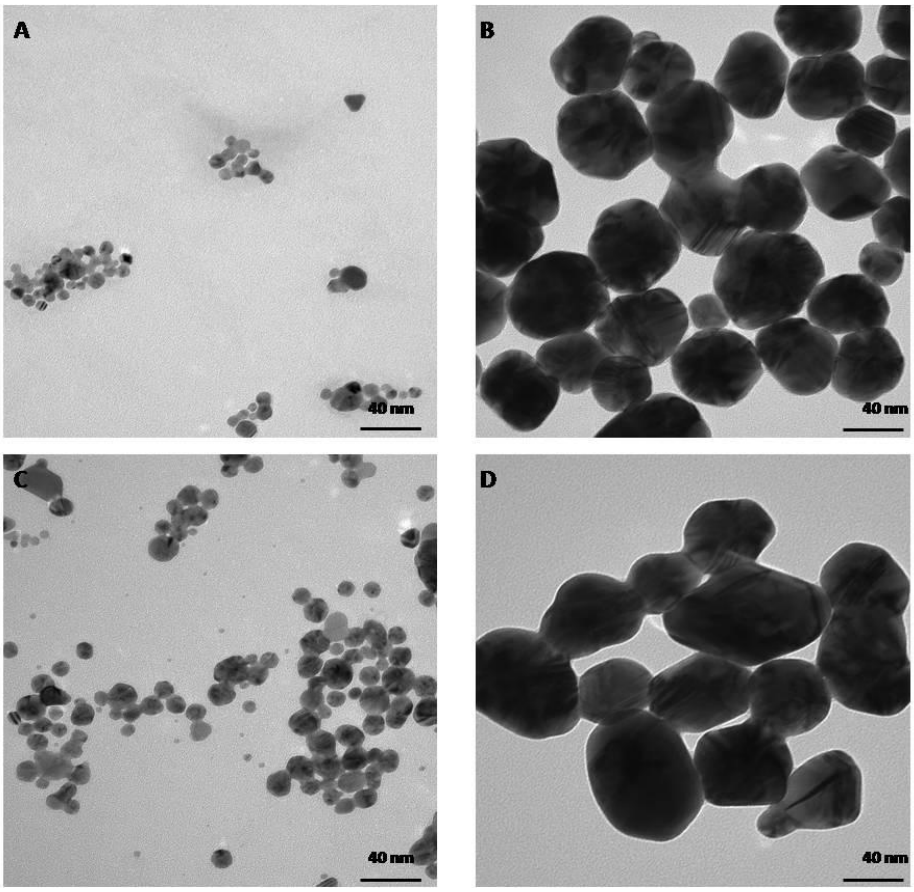

Figure 22. Transmission Electron Microscope Images of Ag Nanoparticles. Images were taken at 100 kV and 100 kx magnification on a formvar-carbon coated Cu grid. (A) Ag 5 nm uncoated. (B) Ag 80 nm uncoated. (C) Ag 10 nm coated. (D) Ag 80 nm coated

Table 4 shows the TEM primary particles size and distribution determined from measurement of over 100 particles from random fields of view. It also shows the DLS z-average particle diameter in solution and LDV zeta potential measurements were measured at sample concentrations of 50 µg/mL of each different nanoparticle used during this study. The results show the average size of the silver nanoparticles. The results show that the smaller nanoparticles, coated 5 nm and uncoated 10 nm, are larger than the size given by the

manufacturer. The 80 nm nanoparticles, coated and uncoated, results indicate that they are smaller than the size given by the manufacturer. The DLS particle diameter in solution indicates that there is little agglomeration in de-ionized water, but an increase in agglomeration when the nanoparticles are in exposure media.

Table 3. Characterization Data for Silver (Ag) Nanoparticles

Particle	TEM Mean Primary Particle Diameter (±SD) (nm)	DLS Z-Average Particle Diameter in Solution (PdI) (nm)		LDV Zeta Potential of Particle Surface Charge (mV)
		DI H2O	*F-12K Media*	*DI H2O*
Ag 5 nm UC	8.9 ± 2.6	30.6 (0.626)	1550 (0.272)	-45.9
Ag 80 nm UC	61.2 ± 15.6	68.8 (0.240)	1710 (0.359)	-13.8
Ag 10 nm C	14.7 ± 4.1	38.7 (0.532)	1930 (0.615)	-37
Ag 80 nm C	65.6 ± 24.0	142 (0.145)	241 (0.400)	-29

4.4. CytoViva™

After exposing the A549 cells to the nanoparticles, photos were taken of the cells using the CytoViva™ method. A control sample was photographed of the A549 cells in exposure media only, shown in Figure 23. Figure 24 shows the cells interaction with the nanoparticles in exposure media. It can be observed through these photos that the nanoparticles do interact with the cell membrane. It is unclear through the use of this method whether the nanoparticles are inside the cells interacting with the mitochondria and the nucleus. Other methods will need to be conducted to determine those interactions.

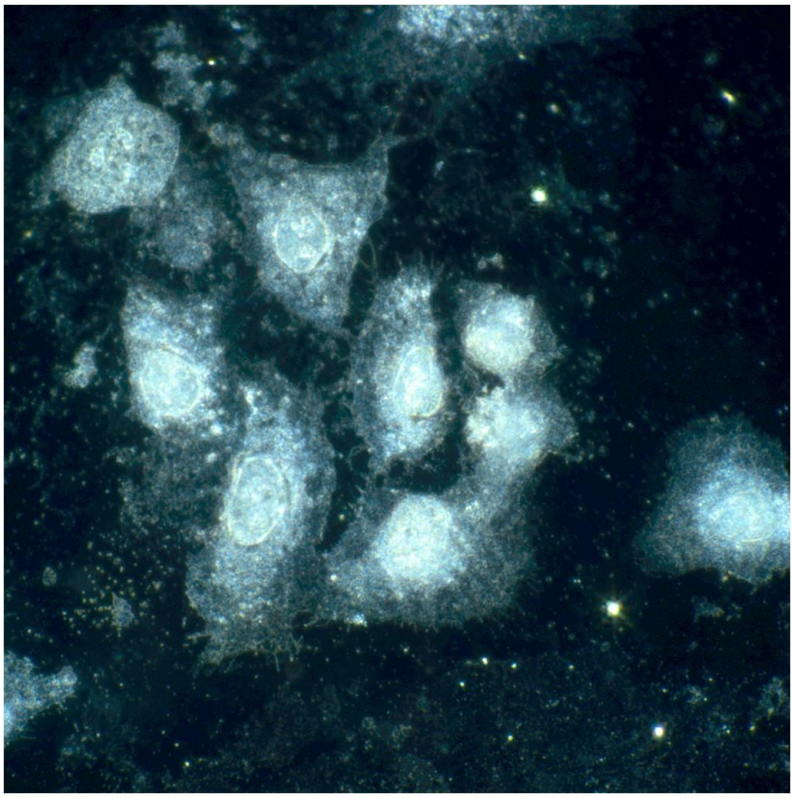

Figure 23. CytoViva™ Picture at 60X (60-times) magnification of the A549 Cells (10 μg/mL solution)

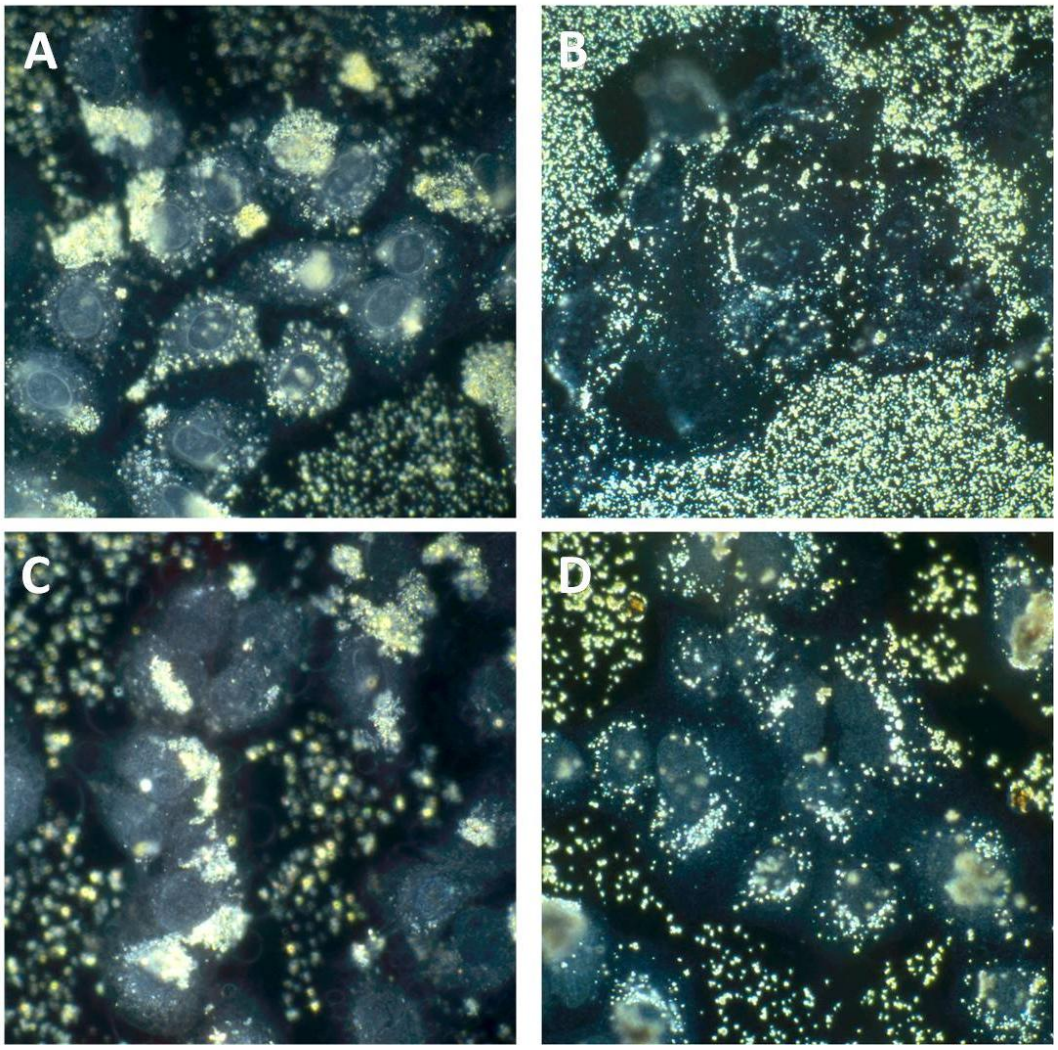

Figure 24. CytoViva™ Pictures at 60X (60 times) magnification of the Silver Nanoparticles and the A549 Cell Line (10 μg/mL solution) – (A) Coated 10 nm, (B) Coated 80 nm, (C) Uncoated 5 nm, (D) Uncoated 80 nm

4.5. Summary

The MTS assay is a reliable assay for determining toxicity of the silver nanoparticles on the A549 cell line. The assay shows that there is both a size and concentration dependence for the level of toxicity to the cell mitochondria. The ROS assay also is a reliable assay for determining the formation of ROS by the silver nanoparticles in the A549 cell line. It also shows a size and

concentration dependent toxicity. Both assays show that the smaller nanoparticles are more toxic to the cells than the larger nanoparticles. The MTS assay shows increasing toxicity with increasing concentration. In contrast, the ROS assay showed a higher formation of ROS with lower concentrations. Both assays also indicated that the uncoated nanoparticles have a higher toxic effect to the cells than the coated nanoparticles. The LDH assay did not provide reliable results for this cell line and the silver nanoparticles.

V. Conclusions and Future Research Considerations

5.1. Overview

This study demonstrates that silver nanoparticles are toxic to epithelial lung cells. Uncoated nanoparticles appear to be more toxic than coated nanoparticles to the lung cell mitochondria. The MTS assay indicates that, with greater concentrations the toxic effects are greater. Also, the MTS assay indicates that the smaller nanoparticles appear to be more toxic than the larger nanoparticles (5 or 10 nm vs. 80 nm) to the cell mitochondria.

The LDH assay was determined to be an unreliable assay to determine toxicity for the silver nanoparticles for this cell line. There is an interference occurring, that would need further investigation.

The ROS assay indicates that the silver nanoparticles do induce the formation of ROS in the cell line. The smaller nanoparticles (uncoated 5 and coated 10 nm) show a higher formation of the ROS in the cells, especially at the lower concentrations 10 and 50 μg/mL. At higher concentrations of these nanoparticles, the ROS formation is lower. The larger nanoparticles, both coated and uncoated 80 nm, show similar results for ROS formation with respect to fold-difference. Although lower than the smaller nanoparticles, they do show formation of the ROS in the cell line.

Both the MTS assay and the ROS assay are reliable assays to determine toxic effects of silver nanoparticles in this cell line. The LDH assay was determined to be unreliable during this study. Both the MTS and ROS assay can

assist in determining toxic effects of the silver nanoparticles in human lung epithelial cells.

Through this study, it can be inferred that there is a mechanism of toxicity through mitochondrial function interference as well as through the formation of ROS within the cell line.

5.2. Investigative Questions Answered

1. Are silver nanoparticles toxic to the A549 (ATCC) lung epithelial cells?

From the MTS assay, it can be interpreted that the silver nanoparticles are, in fact toxic to the A549 lung epithelial cells. The silver nanoparticles affect the mitochondrial activity within these cells negatively. Once the mitochondria in the cells stop functioning, the cells begin to move to apoptosis.

One method in which the nanoparticles cause cells to begin apoptosis is through the formation of reactive oxygen species. These ROS are toxic to the cells and, through the ROS assay, it can be interpreted that the silver nanoparticles cause toxicity to the cells through the formation of ROS. From the results of the ROS assay, it can be determined that the uncoated nanoparticles are more toxic to the cells than the coated nanoparticles. Also, that the smaller of the nanoparticles, whether coated or uncoated, is more toxic to the cell line.

2. Does the exterior coating of the nanoparticles affect toxicity?

By looking at both the MTS assay and the ROS assay, it can be observed that the coating of the nanoparticles does affect the toxicity of the nanoparticle.

The MTS assay indicates that the uncoated nanoparticles are much more toxic than the coated nanoparticles.

This is supported through the ROS assay results. It can be observed that the uncoated nanoparticles are more toxic to the cell line than the uncoated nanoparticles. This is more the case between the smaller of the two types of nanoparticles (uncoated 5 nm and coated 10 nm), than for the 80 nm nanoparticles. The 80 nm nanoparticles show similar formation of ROS with respect to the fold difference with the control across all time points. With the smaller nanoparticles, the uncoated 5 nm shows to have a higher formation of ROS within the cell line, especially in the earlier time points.

3. Does the size difference of the nanoparticles affect toxicity?

By looking at the MTS assay, it is clear that the size of the nanoparticle matters, with respect to its toxic effects. The smaller nanoparticles show a lower percent MTS reduction than their larger counterpart at all concentrations.

This is also supported through the results of the ROS assay. The ROS assay shows that the uncoated 5 nm and coated 10 nm silver nanoparticles induce a greater formation of ROS than the uncoated and coated 80 nm nanoparticles.

5.3. Recommendations for Future Research

As the future of technology shifts into the greater use of the nanoparticles, it is important to acknowledge that these nanoparticles can also cause toxic effects to human health. Future research should include a more in-depth study

into the mechanisms of toxicity. From this study, it can be inferred that toxic mechanisms of silver nanoparticle are through interruption of mitochondrial function as well as the formation of the ROS within the lung cells. The study of lung cells is becoming increasingly important since the silver nanoparticles are being used industrially more than ever; therefore, the inhalation exposure will be increasing. Also, there are products on the market that are aerosol disinfectant sprays that incorporate the use of silver nanoparticles as the disinfectant (Fauss, 2008).

The aerosol use of silver nanoparticles is increasing both in industrial settings and in the public market, understanding the level at which the toxic effects of silver nanoparticles are lethal will be more important than ever. This can also include understanding how this will affect the world of bioterrorism, both in defense and detection. As seen earlier, the DoD, ISN and MIT are delving into the realm of nanoparticle use for the defense and detection. Silver nanoparticles may be able to be used for these types of methods for the warfighter. The knowledge base of its toxicity will need to be built further than its current state.

An assay that can be used in further studies is the apoptosis assay to determine the concentrations and times that apoptosis is occurring. This can be used instead of the LDH assay, which was unreliable in this study. Also, this assay can assist in the further determination of the lethal concentration of silver nanoparticles and at what time point that apoptosis of the cells may occur.

Appendix A: Cell Culturing and Splitting

A549 Cell Line: Human lung epithelial cells, ATCC® (Manassas, VA)

Growth Media: F-12K Medium, Kaighn's Modification of Ham's F-12 with 10% fetal bovine serum (FBS) and 1% Penicillin/Streptomycin (P/S) Solution, ATCC® (Manassas, VA)

PBS: 1% Phosphate Buffer Serum

1. Aspirate culture medium from 75 mL flask.
2. Rinse with 5.0 mL PBS.
3. Aspirate PBS.
4. Add 2.0 mL 0.25% Trypsin with EDTA solution to flask ensuring complete coverage of bottom of flask.
5. Incubate for 4-5 minutes in 37°C incubator, or until the cells have unattached from the bottom of the flask (cells will appear spherical under a light microscope).
6. Add 5.0 mL growth media to flask and break apart the cells by pipetting the solution in and out of the pipette.
7. Count the cells using a standard hemocytometer and light microscope.
    a. Pipette 10 μL of the cell solution onto the hemocytometer
    b. Count cells in each quadrant under a light microscope. The average count from all quadrants indicates the number of cells per milliliter of solution times 10^4.
8. In a new flask add 1.0 mL of the cell culture to 10.0 mL of growth media. Incubate 3-4 days at 37°C.

Appendix B: Cell Growth Curve Procedure

Acidified IPA: solution of 198.36 mL d-H_2O, 1.64 mL concentrated hydrochloric acid (HCl), and 300 mL Isopropyl Alcohol

MTT Solution: 10 mg MTT powder dissolved in 20 mL PBS

1. This procedure is started on a day when the cells are split.
2. In a 6 well culture plate (one for each day of the growth curve duration), add 0.5 mL of a 50,000 cells/mL solution.
3. Incubate each plate for the number of hours/days indicated (24hours/1day, 48hours/2days, etc.).
4. On the day that the plate is read:
    a. For wells 1-3:
        i. Aspirate media.
        ii. Wash each well with 0.5 mL PBS, then aspirate PBS.
        iii. Add 0.25% Trypsin with EDTA solution, incubate 4 - 5 minutes.
        iv. Add 0.5 mL Growth Media to each well, break cells using a pipette.
        v. Mix all 3 wells in a vial and count cells using a hemocytometer.
    b. For wells 4-6
        i. Aspirate media.
        ii. Wash with 0.5 mL PBS and then aspirate PBS.

iii. Add 0.5 mL of MTT Solution to each well, incubate 30 minutes.

iv. Aspirate media. Add 0.5 mL of Acidified IPA to each well.

v. Shake the plate vigorously for 10 minutes on shaker.

vi. Remove 200 μL into a 96-well plate to read absorbance at 490 nm.

5. Record the Cell Count and Absorbance.
6. Repeat as needed over the duration of the Growth Curve Period.

Appendix C: MTT Assay

Exposure Media: F-12K Medium, Kaighn's Modification of Ham's F-12 with 1% Penicillin/Streptomycin (P/S), ATCC® (Manassas, VA)

Acidified IPA: solution of 198.36 mL d-H_2O, 1.64 mL concentrated hydrochloric acid (HCl), and 300 mL Isopropyl Alcohol

MTT Solution: 10 mg MTT powder dissolved in 20 mL PBS

Day 1: Seeding the Cells

1. Follow the procedure for cell culturing.
2. After counting the cells, make a solution that has 200,000 cells/mL in growth media.
3. In a 24 well plate, add 0.5 mL to each well that is being used. Each well was marked with which type of nanoparticle and the dilution factor.
4. Incubate at 37°C for 24 hours.

Table 4. Example of 24-well MTT Plate

	1	2	3	4	5	6
A	BLK	5nm Unctd 100ug/mL	5nm Unctd 200ug/mL	BLK	80nm Uctd 100ug/mL	80nm Uctd 200ug/mL
B	BLK	5nm Unctd 100ug/mL	5nm Unctd 200ug/mL	BLK	80nm Uctd 100ug/mL	80nm Uctd 200ug/mL
C	BLK	5nm Unctd 100ug/mL	5nm Unctd 200ug/mL	BLK	80nm Uctd 100ug/mL	80nm Uctd 200ug/mL
D	BLK	5nm Unctd 100ug/mL	5nm Unctd 200ug/mL	BLK	80nm Uctd 100ug/mL	80nm Uctd 200ug/mL

Day 2: Dosing the Cells

1. Aspirate media from the wells and wash with 0.5 mL per well with PBS.
2. Aspirate PBS.
3. Before adding nanoparticles into solution, sonicate for 10 seconds.
4. Add 0.5 mL of each nanoparticle dosing solution into the appropriate well. Use exposure media to wells with 0 µg/mL nanoparticle solution.

Day 3: MTT

1. Ensure MTT Solution is at room temperature before using.
2. Aspirate media from wells and wash with 0.5 mL per well with PBS.
3. Add 0.5 mL of MTT solution to each well.
4. Cover plates and incubate for 30 minutes for color change.
5. Aspirate media.
6. Add 0.5 mL per well of acidified IPA. Place covered on shaker for 10 minutes to ensure that everything is in solution.
7. Remove 200 µL from each well and transfer to 96 well plate.
8. Read absorbance at 490 nm.

Appendix D: MTS Assay

Exposure Media: F-12K Medium, Kaighn's Modification of Ham's F-12 with 1% Penicillin/Streptomycin (P/S), ATCC® (Manassas, VA)

MTS Solution: CellTiter96® AQ_{ueous} One Solution Reagent for the CellTiter 96® AQ_{ueous} One Solution Cell Proliferation Assay from Promega

Day 1: Seeding the cells

1. Follow the procedure for cell culturing.
2. After counting the cells, make a 23.0 mL solution that has 200,000 cells/mL in growth media.
3. In a 96 well plate, add 200 µL of the cell solution to each well that is being used. Each well should be marked with which type of nanoparticle and the dilution factor.
4. Incubate at 37°C for 24 hours.

Table 5. Example of a 96-Well Plate

	1	2	3	4	5	6	7	8	9	10	11	12
A		blank	10ug/mL 5nm, uc	50ug/mL 5nm, uc	100ug/mL 5nm, uc	200ug/mL 5nm, uc	blank	10ug/mL 10nm, c	50ug/mL 10nm, c	100ug/mL 10nm, c	200ug/mL 10nm, c	
B		blank	10ug/mL 5nm, uc	50ug/mL 5nm, uc	100ug/mL 5nm, uc	200ug/mL 5nm, uc	blank	10ug/mL 10nm, c	50ug/mL 10nm, c	100ug/mL 10nm, c	200ug/mL 10nm, c	
C		blank	10ug/mL 5nm, uc	50ug/mL 5nm, uc	100ug/mL 5nm, uc	200ug/mL 5nm, uc	blank	10ug/mL 10nm, c	50ug/mL 10nm, c	100ug/mL 10nm, c	200ug/mL 10nm, c	
D		blank	10ug/mL 5nm, uc	50ug/mL 5nm, uc	100ug/mL 5nm, uc	200ug/mL 5nm, uc	blank	10ug/mL 10nm, c	50ug/mL 10nm, c	100ug/mL 10nm, c	200ug/mL 10nm, c	
E		blank	10ug/mL 80nm, uc	50ug/mL 80nm, uc	100ug/mL 80nm, uc	200ug/mL 80nm, uc	blank	10ug/mL 80nm, c	50ug/mL 80nm, c	100ug/mL 80nm, c	200ug/mL 80nm, c	
F		blank	10ug/mL 80nm, uc	50ug/mL 80nm, uc	100ug/mL 80nm, uc	200ug/mL 80nm, uc	blank	10ug/mL 80nm, c	50ug/mL 80nm, c	100ug/mL 80nm, c	200ug/mL 80nm, c	
G		blank	10ug/mL 80nm, uc	50ug/mL 80nm, uc	100ug/mL 80nm, uc	200ug/mL 80nm, uc	blank	10ug/mL 80nm, c	50ug/mL 80nm, c	100ug/mL 80nm, c	200ug/mL 80nm, c	
H		blank	10ug/mL 80nm, uc	50ug/mL 80nm, uc	100ug/mL 80nm, uc	200ug/mL 80nm, uc	blank	10ug/mL 80nm, c	50ug/mL 80nm, c	100ug/mL 80nm, c	200ug/mL 80nm, c	

Day 2: Addition of Dosing Solution

1. After 24 hours of incubation, aspirate media out of the plate.
2. Wash with 200 µL of PBS using multi-well pipette. Aspirate PBS.
3. Before adding the nanoparticles into solution, sonicate for 10 seconds.
4. Add 200 µL of dosing solutions or exposure media.
    a. Dosing solutions in accordance with appropriate dilutions.
    b. Exposure media is the control.
5. Incubate 24 hours in 37°C incubator.

Table 6. Dosing solution calculations (1mL Solution)

For a 1 mL Solution:		
Concentration	Exposure Media (mL)	Ag NP (µL of a 1mg/mL solution)
10µg/mL	0.990	10
50µg/mL	0.950	50
100µg/mL	0.900	100
200µg/mL	0.800	200

Day 3: MTS

1. After 24-hour incubation, aspirate exposure media.

2. Wash cells with room temperature PBS 1-2 times to remove any nanoparticles not in the cells.

3. Make a mixture of 20 µL MTS reagent plus 100 µL exposure media for each well.

4. Add 120 µL of the mixture to each well using a multi-channel pipette.

5. Shake gently to mix well.

6. Incubate at 37°C for 1-4 hours (the reagent is yellow and will turn orangey red to dark red depending on the amount of proliferation). It should be checked every hour to determine when it needs to be read.

7. After incubation, put on shaker briefly to ensure that everything is evenly mixed.

8. Read absorbance at 490 nm.

9. Transfer 80 µL of each well to a new plate and read absorbance at 490 nm. This is to ensure that there is no background due to nanoparticles.

Appendix E: Lactate Dehydrogenase (LDH) Assay

LDH Materials: Promega CytoTox 96® Non-Radioactive Cytotoxicity Assay Kit

Exposure Media: F-12K Medium, Kaighn's Modification of Ham's F-12 with 1% P/S, ATCC® (Manassas, VA)

Positive Control: Cadmium Oxide Nanoparticles

Day 1: Seeding the cells

1. Follow the procedure for cell culturing.
2. After counting the cells, make a solution that has 200,000 cells/mL in growth media.
3. In a 96 well plate, add 200 µL to each well that is being used. Each section should be marked with which type of nanoparticle and the dilution factor, to include the positive Control, on the lid.
4. Incubate at 37°C for 24 hours.

Day 2: Addition of Dosing Solution

1. After 24 hours of incubation, aspirate media out of the plate.
2. Wash with 200 µL of PBS using multi-well pipette. Aspirate PBS.
3. Add 200 µL of dosing solutions or exposure media.
    a. Dosing solutions in accordance with appropriate dilutions.
    b. Exposure media is the control.
4. Add 200 µL of positive control solutions into appropriate wells.
5. Incubate 24 hours in 37°C incubator.

Day 3:

1. Remove 50 µL of media from the 96-well plate that has been incubating and place into a new 96-well plate.

2. Add 50 µL of exposure media to each well using a multi channel pipette.

3. Add 50 µL of LDH assay buffer solution into each well. (add 12.0 mL buffer solution to solute powder bottle – in kit)

4. Incubate at room temperature for 30 minutes in the dark (can cover with foil).

5. After 30 minutes add 50 µL of Stop Solution to each well.

6. Read absorbance at 490 nm immediately.

If combining with MTS Assay, also on day 3:

1. After completing the LDH portion of the testing, aspirate the media from the original plate.

2. Wash the wells 3 times with 200 µL PBS using a multi-channel pipette.

3. Add 120 µL of exposure media and MTS solution to each well (100:20 µL ratio).

4. Incubate at 37°C for 1-4 hours, watching for color change.

5. Read absorbance at 490 nm.

6. Remove 80 µL from each well and transfer to new plate. Read absorbance at 490 nm.

Appendix F: Reactive Oxygen Species (ROS) Assay

DCHF-DA: 2',7'– dichlorodihydrofluorescein diacetate, Invitrogen, Lot 478251, 100mg quantities

DMSO: Dimethyl Sulfoxide

Positive Control: 30% H_2O_2 dilutions

Growth/Exposure Media: Dulbecco's Modified Eagle Medium/Nutrient (without Phenol Red) Mixture, F-12 Ham solution was prepared in accordance with the accompanying instructions. The growth media required the addition of 10% fetal bovine serum (FBS) and 1% Penicillin/Streptomycin (P/S) Solution. The exposure media required a 1% Penicillin/Streptomycin (P/S) Solution addition.

1. Seed cells in 96-well black plate (approximately 150,000 cells/mL solution) with 200 µL per well.
2. Incubate at 37°C for 48 hours.
3. Prepare reagents:
    a. DCHF-DA (mw 487.3): 48 mg in 10 mL DMSO = 10 mM
        i. Add 50 µL of stock solution into 5 mL growth media, to yield a 100 µM DCFH-DA solution. For one 96-well plate, a 23 mL solution is needed.
    b. Positive control (H_2O_2)
        i. Add 114 µL of H_2O_2 into 10 mL of PBS to yield a 100 mM Solution of H_2O_2.
        ii. Prepare dosing concentration for positive control in exposure media (500 µM – 2 mM).

4. After incubation, aspirate media from wells and wash with 200 μL PBS for each well.

5. **Under dark conditions**:

a. Add 200 μL of 100 μM DCFH-DA in growth media, incubate 20-30 minutes.

b. Aspirate media with DCFH-DA and wash with 200 μL PBS.

c. Add 200 μL of positive control or dosing solution and cover plates with aluminum foil.

i. Make dosing solution with the required nanoparticle concentrations; e.g. 10 μg/mL, 50 μg/mL, 100 μg/mL
ii. Positive control solution can have differing concentrations of H_2O_2; e.g.10 mM solution, 1 mM solution, 0.1 mM solution, 0.01 mM solution.

d. Read background fluorescence values.

e. Place the plate in the incubator.

f. Measure fluorescence of the cells at excitation 485 nm and emission at 530 nm at specified hour time points (e.g. 1, 4, 6, 24 hours).

g. Remove 80 μL of supernatant from each well and transfer to a new 96-well plate. Read fluorescence.

Bibliography

Alt, V., Bechert, T., Steinrucke, P., Wagener, M., Seidel, P., Dingeldein, E., et al. (2004). An in vitro assessment of the antibacterial properties and cytotoxicity of nanoparticulate silver bone cement. *Biomaterials* , 4383-4391.

Asharani, P., Wu, Y., Gong, Z., & Valiyaveettil, S. (2008). Toxicity of Silver Nanoparticles in Zebrafish Models. *Nanotechnology* , 1-8.

ATCC. (2008). *ATCC product Description.* Retrieved September 29, 2008, from ATCC: http://www.atcc.org/ATCCAdvancedCatalogSearch/ProductDetails/tabid/452/Default.aspx?ATCCNum=CCL-185&Template=cellBiology

Barnard, A. S. (2006). Nanohazards: Knowledge is our first defense. *Nature Materials* , 245-248.

BBWiki. (2007, November 10). Retrieved October 3, 2008, from Lactate dehydrogenase assay: http://bbwiki.tamu.edu/index.php?title=Lactate_dehydrogenase_assay

Berger, M. (2008, June 6). *nanowerk spotlight.* Retrieved June 23, 2008, from nanowerk: http://www.nanowerk.com/spotlight/spotid=5966.php

Biovision. (2008). *LDH kits.* Retrieved October 3, 2008, from Biovision LDH Kits: http://www.biovision.com/LDH-Kits.html?gclid=CPzoILbai5YCFRKIxwodOhBoEg

Boelsterli, U. A. (2007). Xenobiotic-Induced Oxidative Stress: Cell Injury, Signaling, and Gene Regulation. In U. A. Boelsterli, *Mechanistic Toxicology: The Molecular Basis of How Chemicals Disrupt Biological Targets* (pp. 117-169). Boca Raton, Florida: Taylor and Francis Group, L.L.C.

Brown, C. (2003, August 25). *EE Times.* Retrieved October 9, 2008, from EE Times: Nanotech goes to war: http://www.eetimes.com/story/OEG20030825S0017

Buzea, C., & Blandino, R. (2007). Nanomaterials and nanoparticles: Sources and toxicity. *Biointerphases* , MR17-MR172.

Chen, X., & Schluesener, H. (2008). Nanosilver: A nanoproduct in medical application. *Toxicology Letters* , 1-12.

Clarke, B. M. (March 2008). *In Vitro toxicity and inflammatory response induced by copper nanoparticles in rat alveolar macrophages.* Wright-Patterson AFB, OH: School of Engineering Management, Air Force Institute of Technology (AU).

Dallas, C. (2000). Ch 9: Pulmonotoxicity: Toxic Effects in the Lung. In P. Williams, R. James, & S. Roberts, *Principles of Toxicology: Environmental and Industrial Applications* (pp. 169-187). New York: John Wiley and Sons, Inc.

Department of Defense. (2007, April 27). *Defense Nanotechnology Research and Development Program.* Retrieved October 10, 2008, from Defense Nanotechnology: http://nano.gov/html/res/pdf/DefenseNano2007.pdf

Donkin, S. G., Ohlson, D. L., & Teaf, C. M. (2000). Ch 14: Properties and Effects of Metals. In P. L. Williams, R. C. James, & S. M. Roberts, *Principles of Toxicology: Environmental and Industrial Applications* (pp. 325-344). New York: John Wiley and Sons, Inc.

Fauss, E. (2008, September). *The silver nanotechnology commercial inventory.* Retrieved December 11, 2008, from The silver nanotechnology commercial inventory: http://www.nanotechproject.org/process/assets/files/6718/fauss_final.pdf

Fox, S. I. (2006). *Human Physiology.* New York: McGraw-Hill.

Franklin, M., & Yost, G. (2000). Ch 3: Biotransformation: A Balance between Bioactivation and Detoxification. In P. Williams, R. James, & S. Roberts, *Principles of Toxicology: Environmental and Industrial Applications* (pp. 57-86). New York: John Wiley and Sons, Inc.

Gibson, G., & Skett, P. (2001). *Introduction to Drug Metabolism* (3rd ed.). Cheltenham, United Kingdom: Nelson Thornes Publishers.

Goyer, R. A., & Clarkson, T. (2001). Toxic Effects of Metals. In C. Klaassen, *Casarett and Doull's Toxicology: The Basic Science of Poisons* (6th ed., pp. 854-855). New York: McGraw-Hill.

Hussain, S., Hess, K., Gearhart, J., Geiss, K., & Schlager, J. (2005). In vitro toxicity of nanoparticles in BRL 3A rat liver cells. *Toxicology in Vitro* , 975-983.

Jacoby, M. (2003, August 11). *C & EN.* Retrieved October 9, 2008, from C & EN: Cover Story - Science Transforms the Battlefield: http://pubs.acs.org/cen/coverstory/8132/print/8132scienceprint.html

James, R., Roberts, S., & Williams, P. (2000). Ch 1: General Principles of Toxicology. In P. Williams, R. James, & S. Roberts, *Principles of Toxicology: Environmental and Industrial Applications* (pp. 3-34). New York: John Wiley and Sons, Inc.

Koper, O., Klabunde, J., Marchin, G., Klabunde, K., Stoimenov, P., & Bohra, L. (2002). Nanoscale powders and formulations with biocidal activity toward spores and vegetative cells of Bacillus Species, Viruses and Toxins. *Current Microbiology* , 49-55.

Lee, J., Hadjipnanaysis, A., & Parker, M. (2005). Viral Vectors for use in the development of biodefense weapons. *Advanced Drug Delivery Reviews* , 1293-1314.

LePape, H., Solano-Serena, F., Contini, P., Devillers, C., Maftah, A., & Leprat, P. (2004). Involvement of reactive oxygen species in the bactericidal activity of activated carbon fibre supporting silver bactericidal activity of ACF(Ag) mediated by ROS. *Journal of Inorganic Biochemistry* , 1054-1060.

Lu, F., & Kacew, S. (2002). Respiratory System. In F. Lu, & S. Kacew, *Lu's Basic Toxicology: Fundamentals, Target Organs and Risk Assessment* (pp. 168-195). London, England: Taylor and Francis.

Lu, F., & Kacew, S. (2002). Toxicity of Metals. In F. Lu, & S. Kacew, *Lu's Basic Toxicology: Fundamentals, Target Organs, and Risk Assessment* (pp. 302-323). London, England: Taylor and Francis.

Malvern Instruments Ltd. (2005). *Zetasizer Nano Series User Manual, MAN0317.* Worcestershire, UK: Malvern.

Massachusetts Instituite of Technology. (n.d.). *Institute for Soldier Nanotechnologies*. Retrieved October 10, 2008, from MIT: Institute for Soldier Nanotechnologies: http://web.mit.edu/isn/aboutisn/index.html

Moore, M. (2006). Do nanoparticles present ecotoxicological risks for the health of the aquatic environment. *Environment International* , 967-976.

Nanotechnology Characterization Laboratory. (2006, February). *Nanotechnology Characterization Laboratory.* Retrieved October 3, 2008, from HEP G2 Hepatocarcinoma Cytotoxicity Assay: http://ncl.cancer.gov/NCL_method_GTA-2.pdf

National Nanotechnology Initiative. (n.d.). *What is nanotechnology?* Retrieved August 2, 2008, from National Nanotechnology Initiative: http://www.nano.gov/html/facts/whatIsNano.html

Pal, S., Tak, Y., & Song, J. (2007). Does the antibacterial activity of silver nanoparticles depend on the shape of the nanoparticle? A study of the Gram-negative bacterium Escherichia Coli . *Applied and Environmental Microbiology* , 1712-1720.

PennWell Corporation. (2003, May 28). *Small Times.* Retrieved October 9, 2008, from Small Times: U.S. Army has 'big plans' for nanotechnology: http://www.smalltimes.com/articles/stm_print_screen.cfm?ARTICLE_ID=268741

Promega. (2006, August). *Chapter 4: Protocols and Applications.* Retrieved October 3, 2008, from Cell Viability: http://www.promega.com/paguide/chap4.pdf

Promega. (n.d.). *Refinement in the use and data analysis of the promega cellTiter 96 Aqueous Non-radioactive cell proliferation assay*. Retrieved October 3, 2008, from CellTiter96 Aqueous Non-Radioactive Assay: http://www.promega.com/enotes/applications/0004/ap0017.htm

Protocol Online. (2006, September 25). Retrieved October 3, 2008, from Advantages of MTS over MTT: http://www.protocol-online.org/biology-forums/posts/20483.html

Radosavljevic, V. B. (2007). Bioterrorism- Types of Epidemics, new epidemiological paradigm and levels of protection. *Journal of the Royal Institute of Public Health* , 549-557.

Radosavljevic, V., & Jakovljevic, B. (2007). Bioterrorism- Types of Epidemics, new epidemiological paradigm and levels of protection. *Journal of the Royal Institute of Public Health* , 549-557.

Raffi, M., Hussain, F., Bhatti, T., Akhter, J., Hameed, A., & Hasan, M. (2008). Antibacterial Characterization of Silver Nanoparticles Against E.Coli. *Journal of Materials Science and Technology* , 192-196.

Rosner, B. (1990). *Fundamentals of Biostatistics.* Boston: PWS-Kent.

Skebo, J., Grabinski, C., Schrand, A., Schlager, J., & Hussain, S. (2007). Assessment of Metal Nanoparticle Agglomeration, Uptake, and Interaction Using High-Illumination System. *Int. J. of Toxicol.* , 135-141.

Spencer, R. (2007). Potential Bio-Terror Agents. *Journal of Hospital Infection* , 19-22.

Voet, D., & Voet, J. (1995). Electron Transport and Oxidative Phosphorylation. In D. Voet, & J. Voet, *Biochemistry* (pp. 563-598). New York: John Wiley and Sons, Inc.

Wagner, A. J. (March 2006). *In vitro toxicity of aluminum nanoparticles in rat alveolar macrophages.* AFIT/GES/ENV/06M-06. Wright-Patterson AFB, OH: School of Engineering Management, Air Force Institute of Technology (AU).

Wang, H., & Joseph, J. (1999). Quantifying Cellular Oxidative Stress by Dichlorofluorescein Assay Using Microplate Reader. *Free Radical Biology and Medicine , 27*, 612-616.

Xu, Z., Zeng, Q., Lu, G., & Yu, A. (2006). Inorganic nanoparticles as carriers for efficient cellular delivery. *Chemical Engineering Science* , 1027-1040.

Yacobi, N., Harish, P., Demaio, L., Liang, C., Peng, C., Sioutas, C., et al. (2007). Nanoparticle effects on rat alviolar epithelial cell monolayer barrier properties. *Toxicology in Vitro* , 1373-1381.

Yu, K. O. (2008, November 5). Nanoparticle Toxicity. (C. R. Kearns, Interviewer)

REPORT DOCUMENTATION PAGE

Form Approved
OMB No. 074-0188

1. REPORT DATE *(DD-MM-YYYY)*	**2. REPORT TYPE**	**3. DATES COVERED** *(From – To)*
27-03-2009	Master's Thesis	October 2007 – March 2009

4. TITLE AND SUBTITLE

In Vitro Toxicity of Silver Nanoparticles in Human Lung Epithelial Cells

5a. CONTRACT NUMBER

5b. GRANT NUMBER

5c. PROGRAM ELEMENT NUMBER

6. AUTHOR(S)

Kearns, Christina R., CPT, USA

5d. PROJECT NUMBER

5e. TASK NUMBER

5f. WORK UNIT NUMBER

7. PERFORMING ORGANIZATION NAMES(S) AND ADDRESS(S)
Air Force Institute of Technology
Graduate School of Engineering and Management (AFIT/EN)
2950 Hobson Way, Building 640
WPAFB OH 45433-8865

8. PERFORMING ORGANIZATION REPORT NUMBER

AFIT/GWM/ENP/09-M02

9. SPONSORING/MONITORING AGENCY NAME(S) AND ADDRESS(ES)
711 Human Performance Wing/Applied Technology Branch
Bldg 837 'R' Street, Area B
Wright Patterson Air Force Base, OH 45433-5807
Dr. Saber Hussain and Dr. Kyung Yu: 937-904-9504

10. SPONSOR/MONITOR'S ACRONYM(S)
RHPB

11. SPONSOR/MONITOR'S REPORT NUMBER(S)

12. DISTRIBUTION/AVAILABILITY STATEMENT

APPROVED FOR PUBLIC RELEASE; DISTRIBUTION UNLIMITED.

13. SUPPLEMENTARY NOTES

This material is declared a work of the U.S. Government and is not subject to copyright protection in the U.S.

14. ABSTRACT

Nanotechnology is quickly becoming incorporated into everyday products and uses. Silver nanoparticles, specifically, are being used in commercial products, to include aerosols. The purpose of this research was to determine whether silver nanoparticles are toxic to human lung epithelial cells. Different types (coated vs. uncoated), concentrations (10, 50, 100, and 200μg/mL) and sizes (coated 5 and 80nm, uncoated 10 and 80nm) of silver nanoparticles were used during this study. Toxicity measurements were completed through *in vitro* techniques. Another study was also completed on toxicity mechanisms by measuring the reactive oxygen species (ROS) generated. Results showed that silver nanoparticles induce mitochondrial toxicity through a size and concentration dependent manner. Increasing the concentration yielded increased toxicity and the smaller the size induced increased toxicity to the mitochondria. Results also showed that the uncoated nanoparticles were also more toxic to the cells than the coated nanoparticles. The small nanoparticles (coated 5, uncoated 10nm) induced more formation of the ROS than the larger nanoparticles (80nm).

15. SUBJECT TERMS

Nanotechnology, silver nanoparticles, *in vitro,* toxicity, MTS, ROS, bioterrorism, lung cells

16. SECURITY CLASSIFICATION OF:			**17. LIMITATION OF ABSTRACT**	**18. NUMBER OF PAGES**	**19a. NAME OF RESPONSIBLE PERSON**
a. REPORT	**b. ABSTRACT**	**c. THIS PAGE**			**19b. TELEPHONE NUMBER** *(Include area code)*
U	**U**	**U**	**UU**	98	David A. Smith, Lt Col, USAF (ENV) (937) 255-3636, ext 4711 (dasmith@afit.edu)

Standard Form 298 (Rev. 8-98)
Prescribed by ANSI Std. Z39-18